Tanimura A, McGregor DH, Anderson HC (1986b) Calcification in atherosclerosis. II. Animal studies. J Exp Pathol 2:275–297

Thorbecke GJ, Shah R, Leu CH, Kuruvilla AP, Hardison AM, Palladino MA (1992) Involvement of endogenous tumor necrosis factor alpha and transforming growth factor beta during induction of collagen type II arthritis in mice. Proc Natl Acad Sci U S A 89:7375–7379

Tocci MJ, Schmidt JA (1997) Interleukin-1: structure and function. In: Remick DG, Friedland JS (eds) Cytokines in health and disease, 2nd edn. Marcel Dekker, New York, pp 1–27

Van Kooten C, Banchereau J (2000) CD40-CD40 ligand. J Leukoc Biol 67:2–17

Weinberg AD (2002) OX40: Targeted immunotherapy – implications for tempering autoimmunity and enhancing vaccines. Trends Immunol 23:102–109

Werman A, Werman-Venkert R, White R, Lee JK, Werman B, Krelin Y, Voronov E, Dinarello CA, Apte RN (2004) The precursor form of IL-1α is an intracrine proinflammatory activator of transcription. Proc Nat Acad Sci U S A 101:2434–2439

Yao Z, Fanslow WC, Seldin MF, Rousseau AM, Painter SL, Comeau MR, Cohen JI, Spriggs MK (1995a) Herpesvirus Saimiri encodes a new cytokine, IL-17, which binds to a novel cytokine receptor. Immunity 3:811–821

Yao Z, Painter SL, Fanslow WC, Ulrich D, Macduff BM, Spriggs MK, Armitage RJ (1995b) Human IL-17: a novel cytokine derived from T cells. J Immunol 155:5483–5486

Ye P, Rodriguez FH, Kanaly S, Stocking KL, Schurr J, Schwarzenberger P, Oliver P, Huang W, Zhang P, Zhang J, Shellito JE, Bagby GJ, Nelson S, Charrier K, Peschon JJ, Kolls JK (2001) Requirement of interleukin 17 receptor signaling for lung CXC chemokine and granulocyte colony-stimulating factor expression, neutrophil recruitment, and host defense. J Exp Med 194:519–527

Genetically stable and fully effective smallpox vaccine strain constructed from highly attenuated vaccinia LC16m8

Minoru Kidokoro*†, Masato Tashiro*, and Hisatoshi Shida‡

*Department of Virology III, National Institute of Infectious Diseases, 4-7-1 Gakuen, Musashimurayama, Tokyo 208-0011, Japan; and ‡Institute for Genetic Medicine, Hokkaido University, Kita-15, Nishi-7, Kita-ku, Sapporo, Hokkaido 060-0815, Japan

Edited by Peter Palese, Mount Sinai School of Medicine, New York, NY, and approved February 3, 2005 (received for review September 9, 2004)

A highly attenuated LC16m8 (m8) smallpox vaccine has been licensed in Japan because of its extremely low neurovirulence profile, which is comparable to that of replication incompetent strains of vaccinia virus. From 1973 to 1975, m8 was administrated to >100,000 infants where it induced levels of immunity similar to that of the originating Lister strain, without any serious side effects. Recently, we observed that m8 reverts spontaneously to large plaque forming clones that possess virulence equivalent to that of LC16mO, a parental virus strain of m8. Here, we report that the *B5R* gene is responsible for the reversion, and that we could construct a more genetically stable virus by deleting *B5R* from m8. The protective immunogenicity of the vaccine candidate proved to be equivalent to that of the U.S.-licensed product Dryvax, and much superior to modified vaccinia Ankara in a mouse model. Furthermore, the vaccine strain never elicited any symptoms in severe combined immunodeficiency disease mice, even at a dose 1,000-fold greater than that used in the immune protection experiments, which is in contrast to the lethal pathogenicity induced by Dryvax inoculation of severe combined immunodeficiency disease mice. Our results suggest that this vaccine strain is a good candidate as a suitable smallpox vaccine and a vector virus, and that B5R is not essential for protective immunity against smallpox.

B5R gene | reversion | Lister strain | extracellular enveloped virion

Although smallpox was eradicated >20 years ago (1), the necessity of a smallpox vaccine has been reawakened by concerns of bioterrorism using the smallpox virus (2) and outbreaks of monkeypox (3). However, the current vaccine in the United States, Dryvax, occasionally elicits serious adverse effects, including postvaccinal encephalitis (4). Accordingly, a safer smallpox vaccine is much needed.

In Japan, a highly attenuated form of vaccine referred to as LC16m8 (m8) was administrated to >100,000 infants without any serious adverse events and proved to be as immunogenic as the Lister (LO) strain (5, 6), a once widely used vaccine. m8 was indirectly isolated from LO through intermediate strains, such as LC16mO (mO) and LC16. m8, a variant that forms small-sized pocks, is a direct descendant of mO, which itself is a clone that forms medium-sized pocks, isolated from the LC16 strain (5). LC16 was selected from LO based on its temperature sensitivity (5, 7, 8). In rabbit and monkey models, the neurovirulence of m8 was markedly reduced in comparison with other vaccine strains (5, 7–9), including LO and Dryvax (10, 11), and comparable to the replication-defective mutant DIs (Dairen I-derived small-sized pock variant) (12). Moreover, m8 exhibited a markedly diminished dermal reaction in both rabbits and humans and a lower fever ratio compared with mO in clinical trials (5, 6). Therefore, m8 was finally adopted as a vaccine strain instead of mO (6).

Takahashi-Nishimaki *et al.* (13) first identified the vaccinia virus (VV) gene *B5R* as responsible for large plaque formation and proliferating ability in Vero cells. m8 has lost the *B5R* function as the result of a frameshift mutation brought about by a single base deletion in the ORF. *B5R* encodes a 42-kDa glycoprotein that is involved in packaging the intracellular matured virion with trans-Golgi membrane or endosomal cisternae to form an intracellular enveloped virion (IEV) (14–16). IEV is transported along microtubules to the cell periphery (17, 18) where it adheres to the cell surface as a cell-associated enveloped virion (CEV). B5R, in cooperation with the A36R and A33R proteins, also participates in the Src kinase-dependent process of forming of actin-containing microvilli and releasing CEV from the cell surface to form an extracellular enveloped virion (EEV) (19, 20). Despite its relative paucity of whole progeny virions, EEV plays an important role in dissemination within the host (21). Because anti-B5R antibodies can neutralize EEV, expression of *B5R* has been proposed as an effective smallpox vaccine (14, 22–25). In contrast, the results of the field trial in Japan showed that neutralizing (NT) antibody titers induced by m8 were similar to a conventional LO vaccine (5, 6).

Recently, we found that m8 reverted spontaneously to large plaque-forming clones (LPCs).§ The content of LPCs seemed to increase rapidly in proportion to passage number of the virus. Because LPCs emerged from plaque-purified m8, their generation appears to be an intrinsic property of m8. We were concerned that LPC contamination might ruin the safety of the m8 vaccine. Therefore, to improve the m8 strain, we tested whether *B5R* was the gene responsible for the reversion, because this gene has been correlated with large plaque formation. We then constructed genetically more stable virus by deleting *B5R*. Moreover, by using this virus, we were able to evaluate the contribution of *B5R* to protective immunity against smallpox.

Methods

Virus Preparations. m8 was obtained from Chiba Serum Institute (Chiba, Japan). m8rc (plaque-purified m8 to minimize contamination by revertants) and the revertant viruses (LPCs) were isolated from the m8 stock by three serial plaque purifications in RK13 cells. The modified VV Ankara (MVA) (26, 27) and Western Reserve (WR) viruses were obtained from S. Morikawa (National Institute of Infectious Diseases, Tokyo). MVA was propagated and titrated in chicken embryo fibroblasts. Other viruses were propagated and titrated in RK13 cells, and purified by sedimentation through a 36% sucrose cushion. A vial of Dryvax vaccine, obtained from I. K. Damon and J. Becher (Centers for Disease Control and Prevention, Atlanta), was

This paper was submitted directly (Track II) to the PNAS office.

Abbreviations: m8, LC16m8; LO, Lister; mO; LC16mO; VV, vaccinia virus; EEV, extracellular enveloped virion; NT, neutralizing; LPC, large plaque-forming clone; MVA, modified VV Ankara; WR, Western Reserve; PRK, primary rabbit kidney; SCID, severe combined immunodeficiency disease; ED_{50}, 50% erythema dose; RED_{50}, 50% rash expression dose; pfu, plaque-forming units.

†To whom correspondence should be addressed. E-mail: kidokoro@nih.go.jp.

§Kidokoro, M., Eshita, K. & Horiuchi, K., Sixth Meeting of the Japanese Society for Vaccinology (Chiba, Japan), Nov. 30–Dec. 1, 2002, abstr. A-1.

www.pnas.org/cgi/doi/10.1073/pnas.0406671102

dissolved in the enclosed solvent, aliquoted, and stored at −80°C. Construction of m8B5R, which harbors the intact *B5R* gene, m8Δ, which lacks the entire *B5R* gene, and m8dTM, which expresses only the ectodomain of the B5R protein, and characterization of their properties, including the structures of *B5R* in the viruses used, are described in more detail (*Supporting Text*, Table 1, and Fig. 5, which are published as supporting information on the PNAS web site).

Western Blotting. We performed immunoblotting by using an antiserum from rabbits that were immunized with baculovirus-expressed recombinant B5R protein. The anti-B5R sera were used at a dilution of 1:200, and detected with a horseradish peroxidase-labeled secondary antibody and an ECL Plus kit (Amersham Pharmacia Biosciences, Piscataway, NJ).

Evaluation of Genetic Stabilities of VVs. We passaged the VVs in primary rabbit kidney (PRK) cells that are used for vaccine production 7 times at 30°C or 34°C, then in Vero cells 2 times at 34°C to amplify LPCs, or 10 times in PRK at 30°C or 34°C. We estimated the fraction of LPCs as the ratio of plaque counts on Vero cells to those on RK13 cells.

Animals. Severe combined immunodeficiency disease (SCID) mice (female, 6 weeks old) and BALB/c mice (female, 6 weeks old) were purchased from Charles River Japan (Kanagawa, Japan). Female Japan white rabbits (16 weeks old) were obtained from Kitayama Labes (Nagano, Japan). All animal experiments were approved by the National Institute of Infectious Diseases Animal Experiment Committee and were performed in accordance with guidelines for animal experiments performed at the National Institute of Infectious Diseases.

Skin Reaction Test in Rabbits. We conducted a skin reaction test as described (10). Briefly, after inoculating tenfold serial dilutions of VVs intradermally on rabbit backs, the diameters of erythema were measured daily for 1 week. Two animals were used for each viral strain, and each rabbit received two injections of the serial dilution series of a virus. Erythemas >10 mm in diameter was scored as positive. The time at which erythemas reached their peak was determined for each animal, and the 50% erythema dose (ErD_{50}) was calculated by the Beherns and Karber method (28).

SCID Mice Infection Test. To establish an index for pathogenicity of VV against SCID mice, we defined a 50% rash expression dose (RED_{50}), which indicates the virus dose needed to induce a rash in 50% of the animals. After inoculating 10-fold serial dilutions

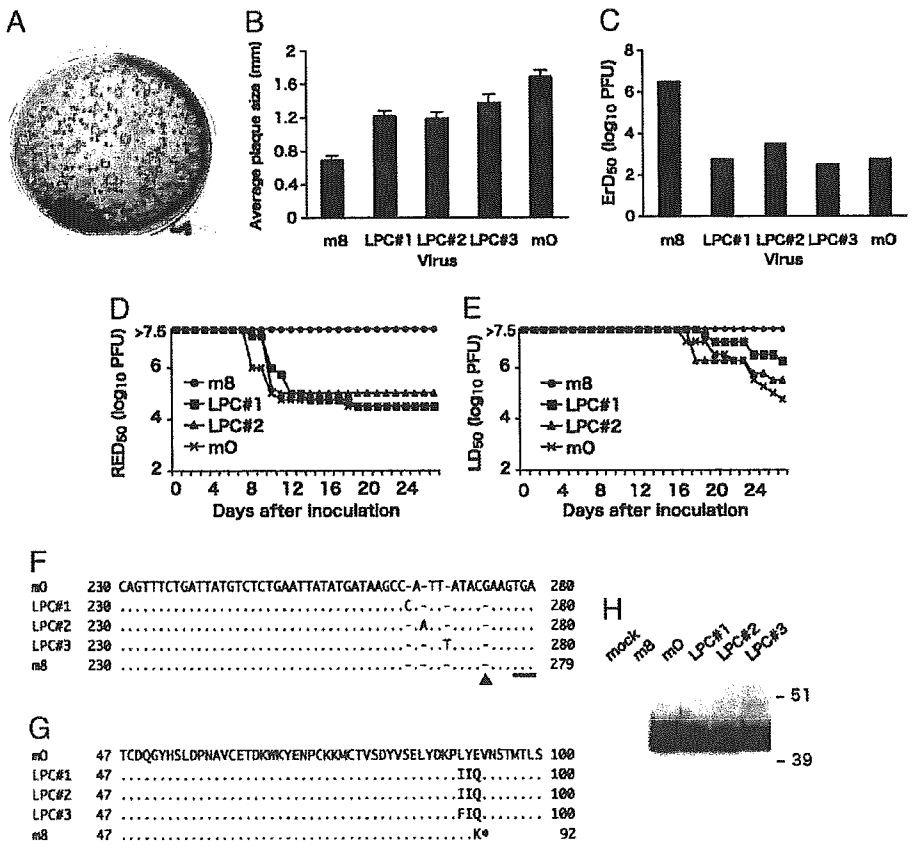

Fig. 1. Biological properties of LPC viruses. (*A*) The plaque configurations of LPCs contaminating an m8 virus stock. LPC viruses make considerably larger plaques than m8. (*B*) The mean plaque sizes of m8, mO, and plaque-purified LPCs. LPCs were isolated from an m8 stock solution. The data are presented as mean ± SD ($P < 0.05$). (*C*) The dermal reaction scores (ErD_{50}) of the LPCs intradermally inoculated in rabbits. (*D* and *E*) Pathogenicity of LPCs against SCID mice. The graphs show temporal changes of RED_{50} (*D*) and LD_{50} (*E*) for a 4-week period after inoculation. The m8 strain was asymptomatic even at the highest viral doses in this experiment (10^7 pfu). If all mice are killed by inoculation of 10^8 pfu of m8, its LD_{50} is $10^{7.5}$ pfu. Therefore, pathogenicity of asymptomatic group ought to be $>10^{7.5}$ pfu. (*F* and *G*) Alignment of the *B5R* nucleotide sequences (*F*) and amino acid sequences (*G*) of mO, m8, and three LPC viruses. Numbers at both ends of the alignments indicate residue numbers. Dots, hyphens, and black triangles in the alignments show identical sequences, gaps, and the single-nucleotide deletion of m8, respectively. The bar and asterisk in the alignments indicate the termination codon. (*H*) Western blots of B5R in VV-infected RK13 cell-lysates. Duplex bands of B5R may be the result of differential glycosylation. Molecular weight markers are shown in kDa.

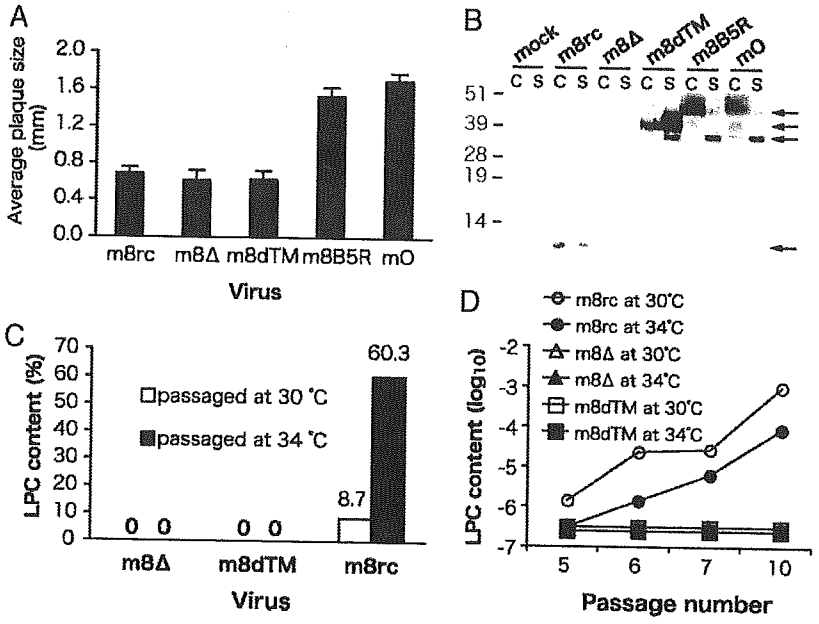

Fig. 2. Characterization of *B5R*-defective viruses. (*A*) The average plaque sizes of m8rc-, m8Δ-, m8dTM-, and *B5R*-positive viruses (m8B5R and mO). The data are presented as mean ± SD. (*B*) Western blots of VV-infected RK13 cell lysates (lane C) and supernatants (lane S). m8rc expresses a short peptide (10 kDa) in the cell and supernatant lanes. The soluble ectodomain of B5R (38 kDa) is expressed from m8dTM. The smaller molecule (35 kDa) in the supernatant lanes of m8dTM, m8B5R, and mO is proteolytically cleaved B5R by cellular proteases. (*C* and *D*) Evaluation of genetic stability by serial passages in PRK and Vero cells under different temperatures (at 30°C or 34°C). The revertant contents of viruses that were passaged seven times in PRK cells and two times in Vero cells are shown in *C*, and those contents that were passaged in PRK cells are shown in *D*.

[10^3 to 10^7 plaque-forming units (pfu)] of VVs i.p. into a series of SCID mice, we calculated the viral doses required for inducing rash (RED_{50}) or killing (LD_{50}) in 50% of the animals by the Reed–Muench method, and followed both values for 4 weeks and 8 weeks.

BALB/c Protection Study. BALB/c mice (eight animals per group) were injected intramuscularly with a single dose of 10^4 to 10^6 pfu of VVs, bled at the tail artery 3 weeks later, and then challenged intranasally with 10^6 pfu of the WR strain 4 weeks after vaccination. Individual body weight was measured daily for 3 weeks, and animals with a weight loss of >30% were killed.

Neutralization Assays. Serial 4-fold dilutions (from 2^{-1} to 2^{-7}) of heat-inactivated mouse serum were mixed with solution containing ≈200 pfu of the WR strain, incubated for 16 h at 37°C, and inoculated on RK13 cells cultured in 48-well plates. Antibody titers were defined as the reciprocal of serum dilution that reduces viral plaques by 50%. All assays were performed in triplicate. The antibody titers of sera from a mock-immunized group were <2 in our assay system.

Statistical Methods. We used Microsoft EXCEL and ORIGIN (OriginLab, Northampton, MA) for statistical analysis. The differences in the mean plaque sizes and in body weight changes measured 5 days after viral challenge in the mouse model were determined by Student's *t* test, with $P < 0.05$ as the criterion for statistical significance. The results are summarized in Table 2, which is published as supporting information on the PNAS web site.

Results

We isolated three LPC clones from an m8 stock and compared several biomarkers with m8 and mO (Fig. 1). All of the clones exhibited phenotypical characteristics similar to mO, such as plaque size (Fig. 1*B*), dermal reactions in rabbits (ErD_{50}) (Fig. 1*C*), and pathogenicity to SCID mice (Fig. 1 *D* and *E*). Specifically, i.p. injection of 10^7 pfu of m8 elicited no overt symptoms over a 4-week period, whereas mO and two LPC clones induced a severe rash and then killed mice, even when administered at a dose (10^5 pfu) 100-fold lower than that of m8 (Fig. 1 *D* and *E*). The accelerated viral replication of LPCs in Vero cells (data not shown) also supported the similarity of the mO and LPC clones. Because the growth ability of mO has been linked to the *B5R* gene product, we hypothesized that the *B5R* gene might be involved in the reversion. Sequencing the LPC genomes revealed that the *B5R* ORF was restored in all of the LPCs, by a one-base insertion at sites just upstream of the deletion site in the m8 *B5R* (Fig. 1 *F* and *G*). Western blotting confirmed the expression of B5R proteins from these LPCs (Fig. 1*H*).

To prevent the reversion of the m8 *B5R* gene, we constructed *B5R*-knockout viruses (see *Supporting Text*). First, we constructed a $B5R^+$ virus (named m8B5R) from m8 by introducing the complete *B5R* cloned from mO (*Supporting Text*, Fig. 5, and Table 1). We then deleted the entire *B5R* sequence from m8B5R to construct m8Δ (*Supporting Text*, Fig. 5, and Table 1). The resultant knockout virus formed plaques as small as the m8rc plaques that were then plaque-purified from m8 stock to minimize LPC contamination (Fig. 2*A*), and did not express the B5R protein in infected RK13 cells, whereas m8B5R and mO did (Fig. 2*B*).

One method by which to augment the immunogenicity of VV without increasing its pathogenicity may be the construction of VV that overexpresses a B5R derivative, which is fully immunogenic but loses its original function in the formation of EEV. The ectodomain of B5R has been reported to possess all epitopes necessary for induction of NT antibody production (22, 29), whereas B5R must be anchored in the membrane for EEV formation (30). We constructed a VV named m8dTM (*Supporting Text*, Fig. 5, and Table 1) that expresses only the ectodomain

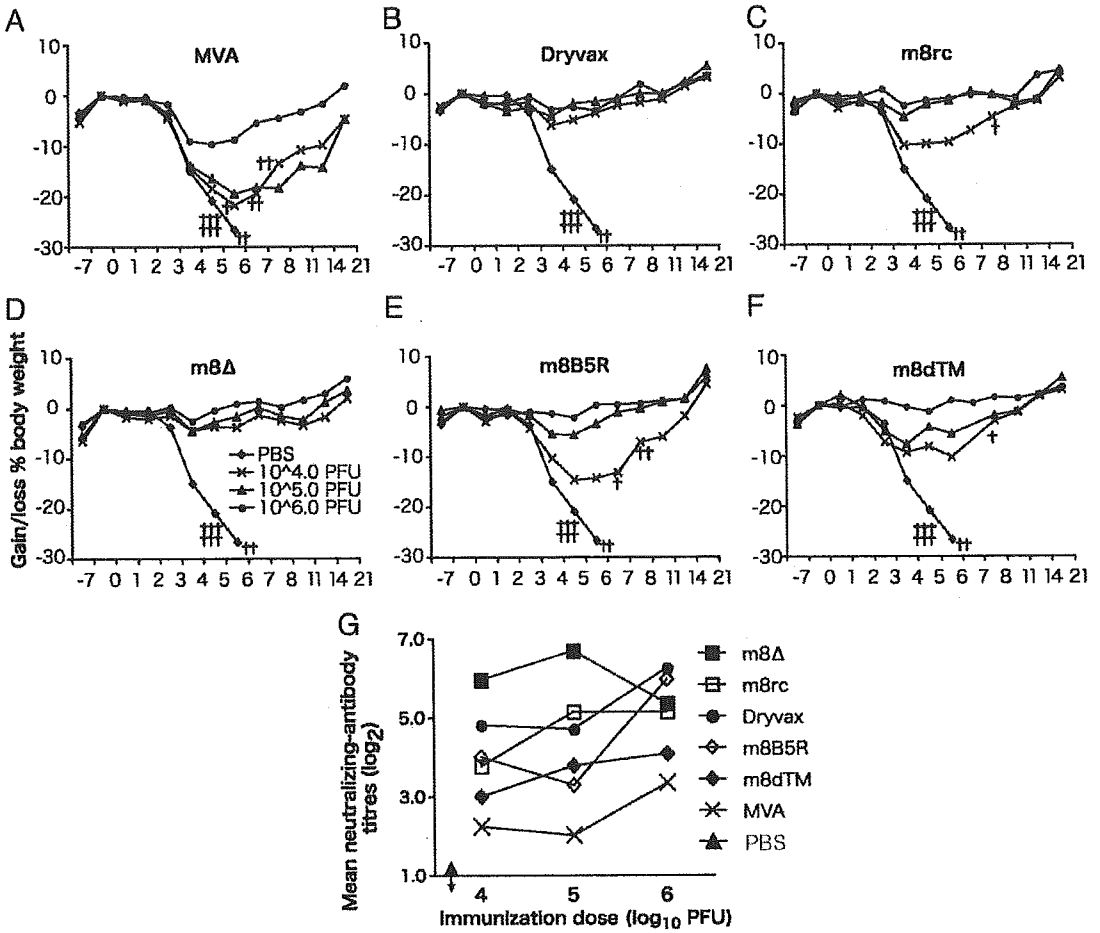

Fig. 3. Protective immunogenicity of vaccine candidate virus in mice. (*A–F*) Average body weight of mice immunized with $10^{4.0}$ to $10^{6.0}$ pfu of VVs intramuscularly and challenged intranasally with the WR strain. Cross marks indicate the mice that died or were killed because of a 30% weight loss. (*G*) Average NT antibody titers in mouse sera collected 3 weeks after immunization with VVs. The titers in sera from a Sham-immunized group were below the limit of detection.

of the B5R protein by replacing the whole *B5R* region of m8B5R with the *B5R* ectodomain sequence placed downstream of the strong promoter PSFJ1–10 (31). m8dTM also formed as small plaques as m8Δ, suggesting that this truncated B5R was not functional for EEV formation. As expected, m8dTM expresses a large quantity of a 38-kDa truncated protein in the culture medium of infected cells (Fig. 2*B*).

To evaluate the genetic stability of the viruses and m8rc, we serially passaged the viruses in PRK cells and Vero cells. Under all conditions tested, including that for vaccine production (passage in PRK cells at 30°C), detectable levels (i.e., levels of $>10^{-6}$) of LPCs failed to emerge from either m8Δ or m8dTM, which is in contrast to the LPC generation from m8rc (Fig. 2 *C* and *D*). Each of the three viruses propagated at similar levels in the cultured cells. It should be noted that once LPCs appeared in the cultures, the fraction of LPCs derived from m8rc rapidly increased with the number of passages (Fig. 2*D*), suggesting it is of vital importance to prevent the emergence of LPCs for optimum quality control of the vaccine.

The protective immunogenicities of smallpox vaccine candidates were compared with other vaccine strains by using a mouse model challenged with a highly pathogenic VV, the WR strain (32) (Fig. 3 and Table 2). All mice immunized with doses of m8Δ or Dryvax survived, whereas all Sham-immunized mice, and 5/8, 3/8, 1/8, and 1/8 mice immunized with 10^4 pfu of MVA, m8B5R, m8rc, or m8dTM, respectively, died or were killed because of a 30% weight loss (Fig. 3 *A–F*). At the lower doses, the mice immunized with m8Δ or Dryvax did not exhibit any significant differences in weight in a challenge after 5 days (*t* test, $P < 0.05$, Table 2). Moreover, the m8Δ-immunized group lost less weight than the Dryvax-immunized group at the highest dose (Table 2). In contrast, the groups immunized with 10^4 pfu of m8rc, m8B5R, and all mice immunized with MVA, experienced a significant weight loss in comparison to m8Δ ($P < 0.05$, Table 2). The m8dTM-immunized group also showed significant weight loss by days 4 and 6 ($P = 0.012$ and 0.038, respectively, data not shown). Measurement of the NT antibody titers elicited in the mice at 3 weeks after immunization (Fig. 3*G*) showed that m8Δ induced the highest titers among the viral strains at lower doses than the other immunizations. The next group, including Dryvax, m8rc, m8B5R, and m8dTM, induced NT antibodies with an efficiency intermediate between m8Δ and MVA. MVA was the least immunogenic virus: 10^6 pfu of MVA was required to induce significant NT antibodies.

The pathogenicity of the *B5R*-defective viruses was examined by ErD_{50} in rabbits (Fig. 4*A*) and by RED_{50} and LD_{50} in SCID mice (Fig. 4 *B* and *C*). m8Δ and m8dTM exhibited an ErD_{50} in rabbits similar to that of m8rc, whereas m8B5R induced the most

MICROBIOLOGY

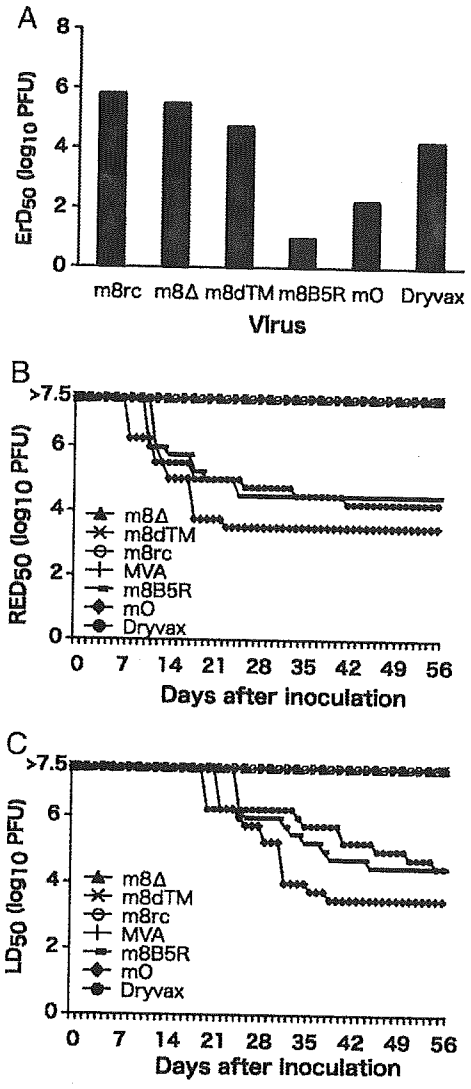

Fig. 4. Pathogenicity of vaccine candidate virus in animals. (*A*) The dermal reaction scores (ErD_{50}) of the *B5R*-defective viruses in rabbits. (*B* and *C*) Virulence of the *B5R*-defective viruses in SCID mice. RED_{50} and LD_{50} are shown in *B* and *C*, respectively.

severe dermal reaction among the strains examined (Fig. 4*A*). The pathogenicity of m8Δ and m8dTM to SCID mice was particularly weak, as demonstrated by the fact that 10^7 pfu of m8Δ or m8dTM did not elicit any symptoms in SCID mice over a period of 56 days (Fig. 4 *B* and *C*). It should be noted that this dose is 1,000-fold higher than that conferring protective immunity (see Fig. 3*D*). MVA and m8rc were also safe in SCID mice, whereas mO, m8B5R, and Dryvax exhibited lethal pathogenicities at lower doses ($10^{3.5}$, $10^{4.5}$, and $10^{4.5}$ pfu, respectively) (Fig. 4 *B* and *C*).

Discussion

One of our goals is to develop a safe and effective smallpox vaccine and vector virus. The m8 strain could be used as a prototype because it has been proven to induce an effective immune response without serious complications in humans (5, 6). It is important to note that the neurovirulence of these strains was separable from their dermal replicability, as suggested by previous experiments with LO-derived strains expressing the envelope protein of human T cell Leukemia virus type 1 (10).

A major safety drawback of m8 is its spontaneous reversion to the mO-like viruses. We identified the *B5R* gene as being responsible for the reversion, and constructed the *B5R*-defective viruses, m8Δ and m8dTM. These viruses are genetically stable and evidently retain the properties of the highly attenuated m8. Moreover, m8Δ shows a level of immunogenicity similar to that of Dryvax.

A previous study (33) reported that the m8-derived recombinant virus, which expresses the hepatitis B surface antigen, maintained its plaque size during 10 passages in the cell culture. The discrepancy between these data and our results in this study may be due to differences in the cell types used to measure plaque sizes. In the earlier study, plaque assays were performed on PRK cell monolayers on which m8 and mO form plaques that are indistinguishable in size, in contrast to the RK13 cell line used in our study. This may be one reason why the reversion of m8 has been previously undocumented.

Another purpose of this study was to evaluate the importance of *B5R* in generating an immune response that confers protection against smallpox infection. B5R protein and a DNA vaccine expressing *B5R* have been reported to induce production of NT antibodies and achieve partial protection against the virus (22–25). Therefore, we assessed the ability of *B5R*, which is expressed during viral replication in mice, to induce protective immunity. The *B5R*-defective virus (m8Δ) was able to elicit NT antibodies, leading to protection comparable to that of the wild-type *B5R*-harboring vaccine, Dryvax. Moreover, the protective efficacies of m8dTM and m8B5R were, unexpectedly, never superior to the *B5R*-defective virus (Fig. 3 and Table 2), and m8B5R was statistically inferior to m8Δ. Western blotting confirmed that B5R proteins were expressed by m8dTM, m8B5R, and Dryvax, and that these proteins were immunogenic and could induce anti-B5R antibody production in mice (data not shown). The subtle difference in protection between m8rc and the *B5R*-knockout virus may be due to the 10-kDa truncated B5R protein synthesized by m8rc (Fig. 2*B*). These data indicate that B5R does not play a major role in inducing protective immunity in response to live vaccinia inoculation in mice. The clinical trial data on m8 in Japan (5, 6) also support our conclusion.

However, the NT antibody titers induced in mice were correlated with body weight changes to some extent, but not completely. Quantitation of antibody titers by ELISAs against the outer membrane proteins of intracellular matured virion (34, 35), which includes L1R, a major target of NT antibodies, showed a similar tendency with NT antibody titers (data not shown). Moreover, the levels of A33R EEV-specific antibodies in mice, which had been suggested to be important for protective immunity (22, 23), did not correlate with the protection level (data not shown). These results may suggest that there may be a contribution of cell-mediated immunities to the protection (36, 37).

Recently, several groups have reevaluated the available vaccinia strains, including the replication-defective MVA, in a search for safer smallpox vaccines (37–40). Although 10^9 pfu of MVA was shown to be safe in monkeys (41), a large quantity of virus, 10^8 pfu, an amount that is 1,000-fold more than a conventional vaccination dosage, was necessary to induce protective immunity (40). Because m8Δ can replicate in the host, it can induce protective immunity comparable to that of the Dryvax strain at a 100-fold lower dose of the virus, making it clearly more effective than MVA. Moreover, m8Δ was not pathogenic in SCID mice at a dose 1,000-fold greater than the lethal dose of Dryvax, a dose that was also 1,000-fold greater than the dose required for its effective protective immunity. m8Δ replicated at the injection site in rabbit skin and caused temporary viremia in SCID mice (data not shown). The preliminary experiments suggested that the viral loads of VV correlate with their pathogenicity to SCID mouse. The virus seems to be eliminated rapidly thereafter and seldom replicates in the CNS (5);

therefore, the magnitude and the region of replication should be restricted, which may explain its safety and efficacy. Therefore, m8Δ should be eminently suitable as a safe and effective vaccine virus and viral vector.

We thank Y. Horiuchi (National Institute of Infectious Diseases) for helpful advice on statistical analysis; S. Morikawa for gifts of anti-B5R rabbit sera and viruses; I. K. Damon and J. Becher for Dryvax vaccine; R. Drillien (Institute of Genetics, Molecular and Cell Biology, Strasbourg, France) and R. Wittek (University of Lausanne, Lausanne, Switzerland) for recombinant baculoviruses; Y. Nagaoka (National Institute of Infectious Diseases) and K. Eshita (Chiba Serum Institute) for technical advice on animal experiments; and H. Yoshizawa, K. Suzuki, and S. Hashizume for sharing information on the basic characteristics of m8.

1. World Health Organization. (1980) *Wkly. Epidemiol. Rec.* **55,** 148.
2. Henderson, D. A., Inglesby, T. V., Bartlett, J. G., Ascher, M. S., Eitzen, E., Jahrling, P. B., Hauer, J., Layton, M., McDade, J., Osterholm, M. T., *et al.* (1999) *J. Am. Med. Assoc.* **281,** 2127–2137.
3. Reed, K. D., Melski, J. W., Graham, M. B., Regnery, R. L., Sotir, M. J., Wegner, M. V., Kazmierczak, J. J., Stratman, E. J., Li, Y., Fairley, J. A., *et al.* (2004) *N. Engl. J. Med.* **350,** 342–350.
4. Centers for Disease Control and Prevention (CDC). (2004) *Morbid. Mortal. Wkly. Rep.* **53,** 106–107.
5. Hashizume, S., Yoshizawa, H., Morita, M. & Suzuki, K. (1985) in *Vaccinia viruses as Vectors for Vaccine Antigens*, ed. Quinnan, G. V. (Elsevier, Amsterdam), pp. 421–428.
6. Yamaguchi, M., Kimura, M. & Hirayama, M. (1975) *Clin. Virol.* **3,** 269–278.
7. Morita, M., Arita, M., Komatsu, T., Amano, H. & Hashizume, S. (1977) *Microbiol. Immunol.* **21,** 417–418.
8. Morita, M., Aoyama, Y., Arita, M., Amano, H., Yoshizawa, H., Hashizume, S., Komatsu, T. & Tagaya, I. (1977) *Arch. Virol.* **53,** 197–208.
9. Kempe, C. H., Fuliginiti, V., Minamitani, M. & Shinefield, H. (1968) *Pediatrics* **42,** 980–985.
10. Shida, H. Hinuma, Y., Hatanaka, M., Morita, M., Kidokoro, M., Suzuki, K., Maruyama, T., Takahashi-Nishimaki, F., Sugimoto, M., Kitamura, R., *et al.* (1988) *J. Virol.* **62,** 4474–4480.
11. Lee, M. S., Roos, J. M., McGuigan, L. C., Smith, K. A., Cormier, N., Cohen, L. K., Roberts, B. E. & Payne, L. G. (1992) *J. Virol.* **66,** 2617–2630.
12. Kitamura, T., Kitamura, Y. & Tagaya, I. (1967) *Nature* **215,** 1187–1188.
13. Takahashi-Nishimaki, F., Funahashi, S., Miki, K., Hashizume, S. & Sugimoto, M. (1991) *Virology* **181,** 158–164.
14. Smith, G. L., Vanderplasschenb, A. & Law, M. (2002) *J. Gen. Virol.* **83,** 2915–2931.
15. Schmelz, M., Sodeik, B., Ericsson, M., Wolffe, E. J., Shida, H., Hiller, G. & Griffiths, G. (1994) *J. Virol.* **68,** 130–147.
16. Hollinshead, M., Rodger, G., Van Eijl, H., Law, M., Hollinshead, R., Vaux, D. J. & Smith, G. L. (2001) *J. Cell Biol.* **154,** 389–402.
17. Rietdorf, J., Ploubidou, A., Reckmann, I., Holmström, A., Frischknecht, F., Zettl, M., Zimmerman, T. & Way, M. (2001) *Nat. Cell Biol.* **3,** 992–1000.
18. Ward, B. M. & Moss, B. (2001) *J. Virol.* **75,** 4802–4813.
19. Katz, E., Ward, B. M., Weisberg, A. S. & Moss, B. (2003) *J. Virol.* **77,** 12266–12275.
20. Newsome, T. P., Scaplehorn, N. & Way, M. (2004) *Science* **306,** 124–129.
21. Payne, L. G. & Kristensson, K. (1985) *J. Gen. Virol.* **66,** 643–646.
22. Galmiche, M. C., Goenaga, J., Wittek, R. & Rindisbacher, L. (1999) *Virology* **254,** 71–80.
23. Hooper, J. W., Custer, D. M. & Thompson, E. (2003) *Virology* **306,** 181–195.
24. Pulford, D. J., Gates, A., Bridge, S. H., Robinson, J. H. & Ulaeto, D. (2004) *Vaccine* **22,** 3358–3366.
25. Hooper, J. W., Thompson, E., Wilhelmsen, C., Zimmerman, M., Ichou, M, A., Steffen, S. E., Schmaljohn, C. S., Schmaljohn, A. L. & Jahrling, P. B. (2004) *J. Virol.* **78,** 4433–4443.
26. Stickl, H., Hochstein-Mintzel, V., Mayr, A., Huber, H. C., Schafer H. & Holzner, A. (1974) *Dtsch. Med. Wochenschr.* **99,** 2386–2392.
27. Mayr, A., Hochstein-Mintzel, V. & Stickl, H. (1974) *Infection* **3,** 6–14.
28. Finney, D. J. (1959) *Acta Microbiol.* **6,** 341–368.
29. Law, M. & Smith, G. L. (2001) *Virology* **280,** 132–142.
30. Herrera, E., Lorenzo, M. M., Blasco, R. & Isaacs, S. N. (1998) *J. Virol.* **72,** 294–302.
31. Jin, N. Y., Funahashi, S. & Shida, H. (1994) *Arch. Virol.* **138,** 315–330.
32. Williamson, J. D., Reith, R. W., Jeffrey, L. J., Arrand, J. R. & Mackett, M. (1990) *J. Gen. Virol.* **71,** 2761–2767.
33. Watanabe, K., Morita, M. & Kojima, A. (1989) *Vaccine* **7,** 499–502.
34. Rodriguez, J. F., Janeczko, R. & Esteban, M. (1985) *J. Virol.* **56,** 482–488.
35. Wolffe, E. J., Vijaya, S. & Moss, B. (1995) *Virology* **211,** 53–63.
36. Xu, R., Johnson, A. J., Liggitt, D. & Bevan, M. J. (2004) *J. Immunol.* **172,** 6265–6271.
37. Wyatt, L. S., Earl, P. L., Eller, L. A. & Moss B. (2004) *Proc. Natl. Acad. Sci. USA* **101,** 4590–4595.
38. Ober, B. T., Bruhl, P., Schmidt, M., Wieser, V., Gritschenberger, W., Coulibaly, S., Savidis-Dacho, H., Gerencer, M. & Falkner, F. G. (2002) *J. Virol.* **76,** 7713–7723.
39. Drexler, I., Staib, C., Kastenmuller, W., Stevanovic, S., Schmidt, B., Lemonnier, F. A., Rammensee, H. G., Busch, D. H., Bernhard, H., Erfle, V., & Sutter, G. (2003) *Proc. Natl. Acad. Sci. USA* **100,** 217–222.
40. Earl, P. L., Americo, J. L., Wyatt, L. S., Eller, L. A., Whitbeck, J. C., Cohen, G. H., Eisenberg, R. J., Hartmann, C. J., Jackson, D. L., Kulesh, D. A., *et al.* (2004) *Nature* **428,** 182–185.
41. Stittelaar, K. J., Kuiken, T., de Swart, R. L., van Amerongen, G., Vos, H. W., Niesters, H. G., van Schalkwijk, P., van der Kwast, T., Wyatt, L. S., Moss, B. & Osterhaus, A. D. (2001) *Vaccine* **19,** 3700–3709.

Available online at www.sciencedirect.com
SCIENCE DIRECT®
ELSEVIER
Microbes and Infection xx (2006) 1–9
Microbes and Infection
www.elsevier.com/locate/micinf

Original article

CRM1, an RNA transporter, is a major species-specific restriction factor of human T cell leukemia virus type 1 (HTLV-1) in rat cells

Xianfeng Zhang [a,1], Yoshiyuki Hakata [a,2], Yuetsu Tanaka [b], Hisatoshi Shida [a,*]

[a] *Institute for Genetic Medicine, Hokkaido University, Kita-15, Nishi-7, Kita-ku, Sapporo 060-0815, Japan*
[b] *Department of Immunology, Graduate School and Faculty of Medicine, University of the Ryukyus, Nishihara, Okinawa 903-0215, Japan*

Received 5 September 2005; accepted 10 October 2005

Abstract

Rat ortholog of human CRM1 has been found to be responsible for the poor activity of viral Rex protein, which is essential for RNA export of human T cell leukemia virus type 1 (HTLV-1). Here, we examined the species-specific barrier of HTLV-1 by establishing rat cell lines, including both adherent and $CD4^+$ T cells, which express human CRM1 at physiological levels. We demonstrated that expression of human CRM1 in rat cells is not harmful to cell growth and is sufficient to restore the synthesis of the viral structural proteins, Gag and Env, at levels similar to those in human cells. Gag precursor proteins were efficiently processed to the mature forms in rat cells and released into the culture medium as sedimentable viral particles. An HTLV-1 pseudovirus infection system suggested that the released virus particles are fully infectious. Our newly developed reporter cell system revealed that Env proteins produced in rat cells are fully fusogenic, which is the basis for cell–cell HTLV-1 infection. Moreover, we show that the early steps in infection, from post-entry uncoating to integration into the host chromosomes, occur efficiently in rat cells. These results, in conjunction with reports describing efficient entry of HTLV-1 into rat cells, may indicate that HTLV-1 is unique in that its major species-specific barrier is determined by CRM1 at a viral RNA export step. These observations will enable us to construct a transgenic rat model expressing human CRM1 that is sensitive to HTLV-1 infection.

Keywords: Human T cell leukemia virus type 1; CRM1; Species barrier

1. Introduction

The human T lymphotropic virus type 1 (HTLV-1) is a type C retrovirus, whose etiological role in adult T cell leukemia (ATL) and tropical spastic paraparesis/HTLV-1 associated myelopathy (TSP/HAM) has been well established [1,2]. In its small genome, the virus encodes not only viral structural and enzymatic proteins, but also several regulatory proteins, using alternative splicing and alternate codon usage. The actions of these regulatory proteins are critical for the virus life cycle. Tax, identified as a viral onco-protein, activates viral and cellular transcription to promote T-cell growth and ultimately, malignant transformation [3,4]. Rex, which is a nucleocytoplasmic shuttling protein, mediates nuclear export of unspliced or incompletely spliced viral mRNAs, which encode the viral structural and enzymatic proteins, Gag, Pol and Env [5–7]. In the nucleus, Rex interacts with the Rex response element (RxRE), which is located in the 3′ long terminal repeat (LTR) of the viral mRNA [8,9]. To form an export complex, Rex binds to human CRM1 (hCRM1), a member of the karyopherin family of nuclear transport receptors, in cooperation with a GTP-bound form of the small G protein Ran (RanGTP) and RanBP3 [10–12]. Moreover, multimerization of Rex on the viral RNA is critical for its full biological activity [13], since the Rex multimer may shield the viral RNA from being spliced or down-regulated [14]. Previously, we reported that hCRM1 is dually involved in both the export of the target

* Corresponding author. Tel./fax: +81 11 706 7543.
E-mail address: hshida@igm.hokudai.ac.jp (H. Shida).
[1] Current address: Retrovirus Research Unit, RIKEN, Wako, Saitama 351-0198, Japan.
[2] Current address: Infectious Disease Laboratory, The Salk Institute for Biological Studies, La Jolla, CA 92037, USA.

1286-4579/$ - see front matter © 2006 Published by Elsevier SAS.
doi:10.1016/j.micinf.2005.10.009

viral mRNA complex and the multimerization of Rex on the cognate RNA [11]. This suggests that hCRM1 is the most critical cofactor guiding Rex function.

Several animal models to investigate the mechanisms underlying the onset of HTLV-1 related diseases have been developed over the past years. Monkeys and rabbits have been used to examine HTLV-1 infection, replication, disease manifestations, immune response, and vaccine development [15–20]. However, rats and mice are more attractive models for HTLV-1 study because of the ease with which they can be genetically manipulated. HTLV-1 transmission to newborn mice has been reported and the HTLV-1 provirus in mouse spleen has been detected [21]. Nevertheless, no viral expression or antibody production was detected in these mice and, furthermore, mouse cells seem to be less susceptible to HTLV-1 envelope fusion [22,23], even though some conflicting results have been reported [24]. In contrast, HTLV-1 infection in rats establishes a persistent infection and elicits specific antibody responses [25,26]. Moreover, HAM/TSP-like diseases develop in HTLV-1-infected WKA/H rats [27,28]. However, until now, efficient replication of HTLV-1 in rat cells has not been reported.

To develop better rat models, it is essential to identify the step at which viral replication is blocked and the host factor(s) responsible. HTLV-1 has been reported to infect several types of rat cells, which indicates that the rat cells possess receptors for viral attachment and penetration [29–31]. Recent identification of a highly conserved molecule, Glut-1, a glucose transporter, as a receptor [32] is consistent with these observations. Previously, we found the inability of the host factor rat CRM1 to support Rex function and thus that viral RNA export from nucleus was a possible block in the viral life cycle. Rat CRM1 induces minimal amount of Rex multimerization on cognate RNA, although it efficiently exports Rex protein to the cytoplasm. This may cause the defect in viral RNA transport [33]. Two residues (amino acids 411 and 414) in the central region of human CRM1 are crucial for multimerization [34]. These results suggest that a transgenic (Tg) rat, which expresses human CRM1, may be a model animal to support replication of HTLV-1. Prior to constructing the Tg rat, we examined the effects of hCRM1, expressed at physiological levels in rat cells, because the above results were obtained by overexpression of human and rat CRM1 and toxic effects from overexpressed CRM1 and a dominant-negative influence of rCRM1 over hCRM1 have been reported [33,35]. Moreover, an understanding of the entire viral life cycle is needed. In the case of the human immunodeficiency virus (HIV), non-human cells have been reported to contain inhibitors such as Trim5α and Apobec3G, which act at uncoating and reverse-transcription steps, respectively [36,37].

In this study, we constructed rat cells expressing hCRM1 at physiological levels and examined the effects on HTLV-1 replication. We investigated the early steps of the HTLV-1 life-cycle, between entry and transcription, and the late steps, including formation of infectious virus and cell to cell infection. To investigate these steps quantitatively, we used a pseudovirus system [38] and our newly devised cell fusion assay, because the extremely poor infectivity of free HTLV-1 virions [38,39] makes it impractical to evaluate them by conventional virological methods. Here, we show that expression of hCRM1 in rat cells may be sufficient to enhance production of HTLV-1 proteins and infectious viruses at levels similar to those in human cells.

2. Materials and methods

2.1. Retro-vector preparation

To construct an hCRM1 expressing retro-vector, the 3 kb fragment, which encodes the 3′ part of the hCRM1 coding frame, was isolated from pSRαhCRM1 plasmid [11] by digestion with AatII and XhoI, and the left 5′ part was amplified by PCR using the primer pair: hCrm15′F: CCG AAT TCT CTC TGG TAA TCT ATG CCA GCA A; hCrm15′R: CAA GTT GGG TCA GAT GAC GTC TT on pSRαhCRM1 as a template. The PCR was performed by a single step of 94 °C for 90 s and 10 cycles of a three-temperature PCR (94 °C for 30 s, 56 °C for 60 s, and 72 °C for 30 s) followed by one step of 72 °C for 5 min. The amplified fragment was then digested with AatII and EcoRI. The two fragments of hCRM1 cDNA were then ligated to retrovector pMX-neo digested with EcoRI and XhoI [40]. The resultant expression plasmid, named pMXneohCRM1, was transfected to packaging PLAT-E cells, the supernatants were collected, and stored at −80 °C.

2.2. Construction of stable cell lines

Rat mammary adenocarcinoma ER-1 cells, maintained in Dulbecco's modified Eagle's medium (DMEM, Sigma, St. Louis, MO) supplemented with 10% fetal bovine serum (FCS), were seeded into 6-well plates at a density of 1×10^5 cells/well 1 day before infection. To construct stable rat cell lines which express hCRM1, ER-1 cells were incubated with 0.5 ml of MXneohCRM1 virus solution for 4 h in the presence of 10 μg/ml polybrene, and then fresh medium was added. The hCRM1 expressing clones were selected in the presence of 300 μg/ml neomycin. We picked two neomycin resistant clones and designated them ER-1/hCRM1-1 and ER-1/hCRM1-2, respectively. The control cells, designated as ER-1neo1, were infected with virus carrying the MX-neo plasmid.

To construct an hCRM1 expressing rat T cell line, 1×10^5 FPM1 cells, an HTLV-1 transformed rat $CD4^+$ T cell line, were infected with MXneohCRM1 and selected with 100 μg/ml neomycin. The resistant cells were then divided into 96-well plates at 0.1 cells per well to clone the FPM1hCRM1-14 line.

To establish reporter cells for detection of HTLV-1-induced cell fusion, 5×10^5 293T cells in 10 cm petri dishes were transfected with 2.5 μg of pLTR-GL3 [14] and 0.5 μg of pTK-Hyg (Clontech, Palo Alto, CA) using Lipofectamine Plus (Invitrogen, Carlsbad, CA), according to the manufacturer's instructions. Forty-eight hours after transfection, the medium was replaced with fresh DMEM supplemented with

10% FCS and 300 μg/ml hygromycin B. Antibiotic resistant colonies were picked with a cloning cylinder. A cell clone, designated as 293T/LTR-Luc8, was used in this study.

2.3. Measurement of Rex activity

The cells (1×10^5) were transfected with 0.4 μg of pDM128RxRE [33], 0.05 μg of pSRαRex, and 0.1 μg of pCDMβ-Gal. Twenty-four hours after transfection the cells were lysed and the amount of CAT was quantified using a CAT ELISA kit (Roche). The β-galactosidase (β-gal) activity was measured by standard colorimetric methods, to normalize the transfection efficiency. The Rex activity was represented by a ratio of CAT/β-gal for each sample as described previously [33].

2.4. Measurement of HTLV-1 Gag production

The human and rat cell lines (1×10^5) were transfected with 0.5 μg of HTLV-1 infectious clone K30 and 0.1 μg of pCDMβ-Gal. Forty-eight hours after transfection, the medium of the cell culture was harvested and centrifuged at low speed to remove the cell debris. The transfected cells were washed twice with PBS then scraped off and transferred to microcentrifuge tubes; the cells were suspended in 50 μl of lysis buffer (10 mM Tris—HCl, 140 mM NaCl, 3 mM $MgCl_2$, 1 mM DTT, 0.5% NP-40, 1 μg/ml of aprotinin, leupeptin and pepstain). Gag was quantified by a RETRO-TEK HTLV-1 p19 Gag ELISA kit according to the manufacturer's protocol.

2.5. Immunoblot analysis

Immunoblot analysis was performed for detection of CRM1 using affinity purified chicken anti- hCRM1 and rabbit anti-rCRM1 antibodies [33]. To detect HTLV-1 proteins, we used rabbit anti Rex antisera, mouse anti-Tax MAb Lt-4, and mouse anti-p24 Gag MAb NOR-1 [42]. To detect the HTLV-1 Env protein, we concentrated the Env proteins using Concanavalin A (Con-A) Sepharose and then detected with rat anti-gp46 MAb LAT-27 [43]. For detection of Gag in released virions, the culture medium was ultracentrifuged at 40,000 rpm for 1 h in a Beckman TLA100.3 rotor at 4 °C. The pellets were suspended in the sample buffer and processed for immunoblotting. To detect the HTLV-1 Env protein in the cell lysate, 5×10^5 rat or human cells in 10 cm petri dishes were transfected with 2.5 μg of HTLV-1 K30. The cells were lysed 48 h after infection and applied to Con-A Sepharose. The concentrated glycoproteins were eluted using sample loading buffer.

2.6. Quantification of fusion activity of HTLV-1 infected cells

The infectious clone HTLV-1 K30 (0.5 μg) was used to transfect various rat and human cells, and 24 h later the cells were trypsinized and suspended in fresh medium. The cells were mixed with an equal number (1×10^5) of 293T/LTR-Luc8 cells, and cultured for an additional 48 h. The cells were lysed and luciferase expression measured using the Steady-Glo luciferase assay system (Promega, Madison, WI) to evaluate fusion activity.

2.7. Cell free infection and gene transduction analysis

The preparation of pseudotyped HTLV-1 virus and virus infection were performed, as described previously, except that the reporter plasmid, pHTC-GFP-Luc was used instead of pHTC-Luc-tsa [38]. pHTC-GFP-Luc, a newly developed reporter vector by David Derse's group, encodes a GFP-luciferase fusion protein, otherwise identical to pHTC-Luc-tsa. Briefly, pCMVHT-Δenv and pHTC-GFP-Luc, which were kindly provided by Dr David Derse, and pMD-VSV-G were transfected into 1×10^6 cells. The culture supernatant, which contains resultant viruses, was harvested 28 h after transfection and used to infect various cell types. Seventy-two hours later luciferase activity in the infected cells was measured. For AZT inhibition, 100 nM of 3′-azido-3′-deoxythymidine (AZT) (Sigma) was used to treat the infected cells as described [38].

3. Results

3.1. Effects of hCRM1 expressed in rat adenocarcinoma cell lines

We first established the stable rat adenocarcinoma cell lines, ER-1/hCRM1-1 and -2, which express hCRM1, by transduction with MxneohCRM1, a retro-vector encoding the hCRM1 cDNA. A control cell line named ER-1neo1, which carries only the neomycin resistance gene, was also generated. ER-1/hCRM1-1 and ER-1/hCRM1-2 expressed hCRM1 at levels similar to human HeLa cells and CD4-HeLa cells, as judged by immunoblotting. hCRM1 was not detected in the parental ER-1 or control ER-1neo1 cell samples (Fig. 1A). Both cell lines expressing hCRM1 propagated similarly or a little faster than parental ER-1 (Fig. 1B). It is conceivable that double the amount of CRM1in the hCRM1 expressing rat cells, which also express rat CRM1, might facilitate rat mRNA/protein export, leading to better growth. However, it is less likely, because ER-1 neo1 grew equally well as the hCRM1 expressing ER-1 cells. In any case our results suggest that expression of physiological levels of hCRM1 does not negatively affect the replication dynamics of cells.

Next, we examined whether the hCRM1 transgene can restore Rex activity in rat cell lines. We co-transfected a CAT expressing reporter, the pDM128RxRE, pSRαRex, and pCDMβ-gal plasmids, and quantified Rex activity based on the amount of CAT protein production. In the parental rat ER-1 and control ER-1neo1 cells, Rex activity was undetectable, while in the hCRM1-expressing cells Rex activity was significantly augmented to levels found in HeLa and CD4-HeLa cells (Fig. 1C). As predicted, CAT expression in cells transfected only with pCDM128RxRE was very low. These results clearly demonstrate that expression of hCRM1 in rat cells

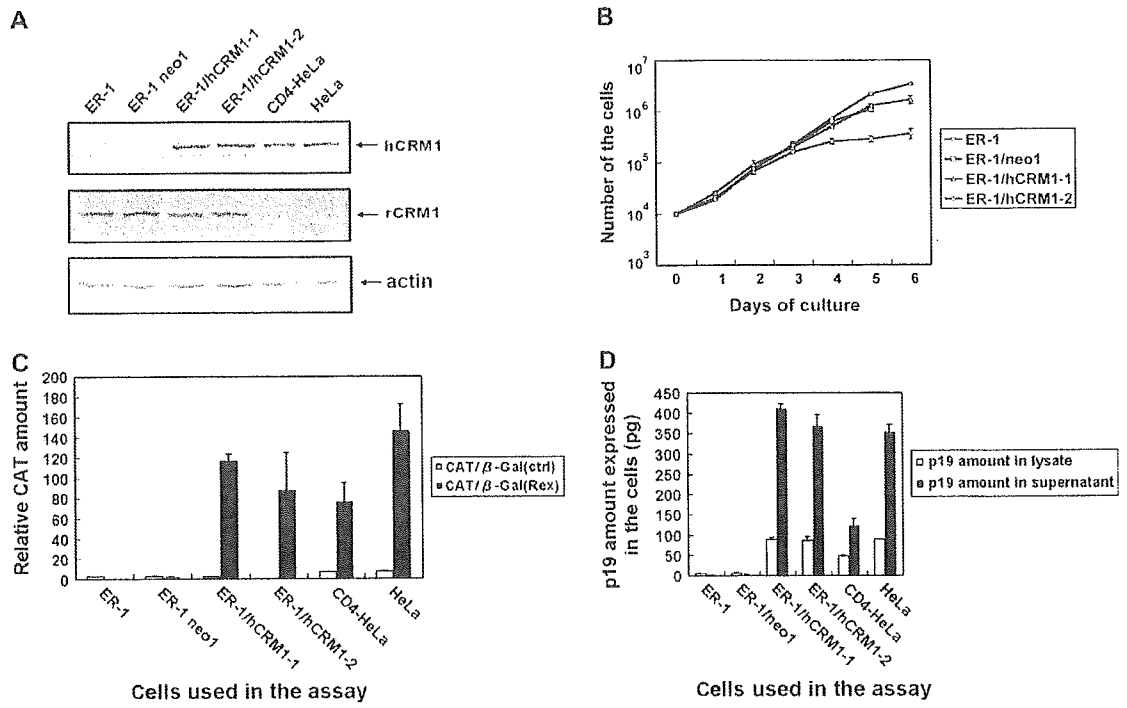

Fig. 1. Properties of hCRM1 expressing adherent rat cell lines. (A) The rat mammary tumor cell line, ER-1, was transduced with the retrovector Mx-neo-hCRM1 or Mx-neo. The expression of hCRM1 and rCRM1 in the selected clones as well as the parental rat cell and control human cell lines was examined by immunoblotting. The same amounts of the cell lysates were loaded on the SDS-PAGE. The expression of β-actin was also examined as a control to monitor the amounts of samples applied in the assay. (B) The cell growth of hCRM1-transduced rat cell clones was compared with parental ER-1 The cells (1×10^4/ml) were seeded into a 6-well plate, and counted every 24 h. (C) hCRM1 expression enhances Rex activity in rat cells. The results are shown as the means of three independent experiments. (D) hCRM1 augments HTLV-1 Gag production in the rat cells. The rat and human cell lines were transfected with the HTLV-1 K30 and Gag products in the cell lysate and culture medium were quantified by HTLV-1 p19 ELISA. The results are shown as the mean of three independent experiments.

is sufficient to augment Rex activity to levels similar to those found endogenously in human cells, regardless of the presence of endogenous rCRM1.

The restoration of Rex activity may directly result in enhanced expression of the HTLV-1 viral structural protein. To test this possibility, we transfected rat and human cells with the HTLV-1 molecular clone K30. Gag production was first quantified using an HTLV-1 p19 antigen ELISA (Fig. 1D). The p19 antigens were produced at similar levels in hCRM1 expressing rat and human cells, whereas very low levels of p19 were detected in the parental ER-1 and control ER-1neo1 samples. The ratio of p19 in the medium to that in the cell lysate was 3–4 in both human and rat cells expressing hCRM1. Approximately 30% of the secreted Gag protein, which was produced in all types of hCRM1 expressing cells, could be pelleted by ultracentrifugation (Table 1). Taken together, these results suggest that viral particles budded from rat cells as efficiently as human cells.

To further examine the expression of the HTLV-1 structural proteins in rat cells expressing hCRM1, we performed a Western blot analysis (Fig. 2). Gag proteins including p24 and its precursor p55 were expressed equally well in human and rat cells expressing hCRM1, but were not expressed in control ER-1neo1 rat cells. The efficiency of processing p55 to p24 was similar in human and rat cells and the p38 intermediate was detected in both cell lines. Similar amounts of the HTLV-1 gp46 Env protein and its precursor gp61 were detected in both human and rat cells expressing hCRM1, but not in control ER-1neo1 rat cells. In contrast, the two trans-regulatory proteins, Tax and Rex, were expressed at similar levels in all rat and human cells upon HTLV-1 K30 transfection.

Since it is difficult to measure the infectivity of HTLV-1 by conventional methods, we applied a reporter virus assay [38], in which the HTLV-1 pseudovirus harboring a luciferase gene is coated with G proteins of vesicular stomatitis virus (VSV), which shows a broad tropism. Luciferase is driven by the

Table 1
Amount of HTLV-1 p19 Gag protein in K30-transfected rat and human cells[a]

	P19 amount (pg) in		
Cells	Culture medium	Concentrated pellet	Lysate
ER-1	UD[b]	UD	UD
ER-1/neo1	UD	UD	UD
ER-1/hCRM1-1	412 ± 12	116 ± 5	89 ± 6
ER-1/hCRM1-2	369 ± 27	122 ± 9	87 ± 13
CD4-HeLa	122 ± 18	41 ± 1	48 ± 5
HeLa	355 ± 17	96 ± 2	90 ± 5

[a] Cells (1×10^5) were transfected with 0.5 μg of the HTLV-1 K30. Forty-eight hours after transfection, the cells and medium of the culture were harvested and applied to HTLV-1 p19 ELISA. The total amount of p19 was calculated. The results are shown as the mean of three independent experiments.
[b] UD, under detection limit.

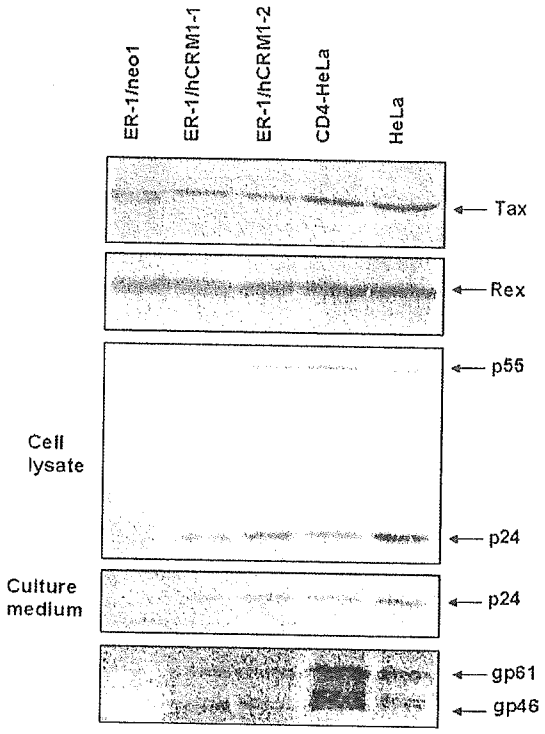

Fig. 2. hCRM1 enhances expression of HTLV-1 structural proteins, but not regulatory proteins, in rat cell lines. HTLV-1 K30-transfected cells and their culture medium were harvested and immunoblot assays were performed to detect the expression of viral proteins. The amount of samples was normalized by transfection efficiency based on β-galactosidase activity before applying to SDS-PAGE. The samples for detection of Gag in released virions and Env protein in the cell lysate were prepared as described in Section 2.

strong CMV promoter, and used as a sensitive marker of the gene expression from viral genomes, which have integrated into their host cells. We produced the pseudotyped viruses in ER-1/neo1, ER-1/hCRM1-2, HeLa and CD4-HeLa cell lines, and compared their luciferase inducing capacity after infection of 293 cells (Table 2). The pseudovirus produced in ER-1/hCRM1-2 or CD4-HeLa induced similar levels of luciferase activity, which was greater than that produced by HeLa cell derived pseudoviruses. The luciferase activity was positively correlated to the amount of HTLV-1 p19 in the medium. The luciferase activity from ER-1neo1 samples represents the background. The luciferase activity was reduced to background levels by AZT, an inhibitor of the viral reverse transcriptase, indicating that the infection occurred through the normal retrovirus infection route. These results suggest that HTLV-1 virions produced from the hCRM1 expressing rat cells are fully infectious.

3.2. hCRM1 expression converts rat CD4$^+$ T cells into high efficiency HTLV-1 producers

To examine the effect of hCRM1 expression in rat CD4$^+$ T cells, we transduced MXhCRM1 into FPM1, an HTLV-1-transformed rat CD4$^+$ T cell line (Fig. 3). The FPM1-derived

Table 2
Infectivity of pseudotyped HTLV-1 produced in rat and human cells[a]

Cells	Luciferase activity in infected 293 cells		p19 ELISA titer (pg/ml)
	Without AZT	With AZT	
ER-1/neo1	239[b]	261	UD
ER-1/hCRM1-2	1654	265	638
HeLa	444	132	347
CD4-HeLa	1729	370	1219

[a] The pseudotyped viruses produced in various cells were quantified by p19 ELISA and infected to 293 cells in the absence or presence of AZT. Seventy-two hours later luciferase activity in the infected cells was measured. Representative results of two independent experiments are shown.
[b] RLU, relative light units.

hCRM1 expressing cells, FPM1-hCRM1-14, produced hCRM1 levels comparable to the Jurkat human T cell line and to MT-4, an HTLV-1 producing human T cell line. FPM1-hCRM1-14 grew as well as the parental FPM1 cells (Fig. 3A). FPM1 has been reported to selectively express viral regulatory proteins, such as Tax, but not structural proteins [44]. Our ELISA data consistently showed very low levels of p19 expression (approximately 25 pg/ml) in the culture medium of FPM1, whereas FPM1-hCRM1-14 produced very high levels of secreted Gag antigen (approximately 7400 pg/ml), comparable to MT-4 cells (data not shown).

Western blotting showed that expression of hCRM1 in FPM1 did not affect the amount of Tax and Rex proteins, which are encoded by mRNAs that are exported independently of CRM1. In contrast, hCRM1 augmented the production of Gag and Env proteins. The Gag precursor p55 was processed to mature p24 as efficiently as the human T cells (Fig. 3B).

3.3. Fusion ability of HTLV-1-infected rat cells

Efficient spread of HTLV-1 requires cell contact [45,46]. Lymphocytes naturally infected with HTLV-1 produce very few cell-free HTLV-1 virions, and one in 10^5 to 10^6 virions is estimated to be infectious [38,39]. The cell-to-cell spread of HTLV-1 is mediated through fusion of the two cell membranes caused by Env proteins [23,47,48]. Certain integrins, including the intercellular and vascular cell adhesion molecules ICAM-1, ICAM-3, and VCAM, act as cofactors for HTLV-1-induced cell fusion [49,50]. To quantify the fusion efficiency of HTLV-1-infected cells, we established a 293T derived reporter cell, 293/LTR-luc8, which harbors an HTLV-1 LTR promoter-driven luciferase reporter gene. When cell fusion occurs following co-culture of this reporter cell with HTLV-1 producing cells, Tax protein is transferred from the donor cells and activates the LTR promoter. An alternative route to activate the luciferase gene is through newly synthesized Tax protein from an HTLV-1 genome, which has been transferred from the donor cells, reverse-transcribed, and integrated into a reporter cell chromosome. In either case, the fusion ability of the HTLV-1 infected cells can be evaluated by luciferase expression. The reporter cells express very low levels of luciferase under normal culture conditions,

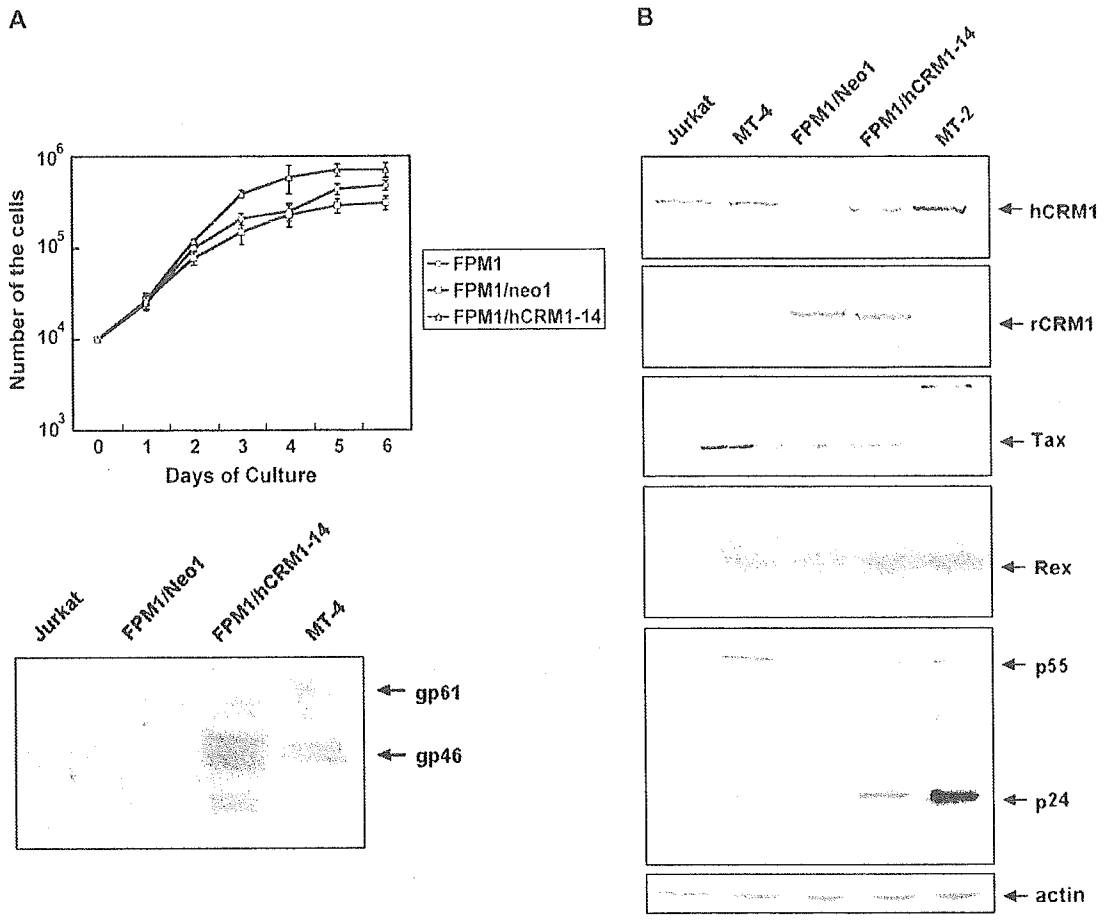

Fig. 3. hCRM1 enhanced viral structural protein expression in HTLV-1-infected rat T-cell lines. (A) The cell growth of hCRM1-transduced rat T cell clones was compared with parental FPM1 cells. The cells (1×10^4/ml) were seeded into a 6-well plate, and counted every 24 h. (B) HTLV-1-infected and uninfected rat and human T cells (1×10^6 cells) were harvested in their log growth phase. Immunoblotting was performed as in Fig. 1A and Fig. 2. The expression of β-actin was also examined as a control to monitor the amounts of samples applied in the assay.

but have a very sensitive LTR response upon Tax stimulation, as demonstrated by transient expression of a Tax encoding plasmid (data not shown), or co-culture with as few as 1×10^3 HTLV-1 producing MT-2 cells. Luciferase activity increased linearly with the number of MT-2 cells, up to 5×10^4 cells. In contrast, co-culture with 5×10^4 Jurkat cells did not induce luciferase activity (Fig. 4A).

To compare the fusion capability of virus-producing cells, we first transfected various rat and human cells with HTLV-1 K30, incubated the cells for 24 h after transfection, and then co-cultured them with 293T/LTR-luc8 cells for a further 72 h. As shown in Fig. 4B, the luciferase activity induced by co-culture with ER-1/hCRM1-1 and ER-1/hCRM1-2 was as high as that resulting from co-culture with HeLa or CD4-HeLa cells, as well as the HTLV-1 high producing line C77, suggesting that K30-infected rat cells could be highly infectious. In contrast, the luciferase expression in reporter cells co-cultured with ER-1neo1 was close to the basal level. As a control, rat and human cells transfected with a Tax expressing plasmid pSRαTax in the absence of Env expression were also unable to increase luciferase expression when co-cultured with 293T/LTR-luc8 cells (data not shown), indicating that luciferase expression depends on cell fusion mediated by Env proteins.

The fusion ability of HTLV-1-infected rat T cells was also investigated. The luciferase level in reporter cells co-cultured with both human T cells (MT-4) and FPM1-mxhCRM1-14 were unexpectedly lower than the adherent cells described above. Nevertheless, the hCRM1 expressing rat T cells stimulated luciferase activity more efficiently than MT-4 cells (Fig. 4C). Luciferase activity was proportional to the amount of Env gp46 expressed (see Figs. 3 and 4). These results clearly demonstrate that the Env protein induced by hCRM1 in the rat cells is fully fusogenic, supporting HTLV-1 infectivity in rat cells.

To discriminate whether a Tax protein transferred from the donor cells or Tax protein produced from the HTLV-1 genome which had infected the reporter cells was the primary inducer of luciferase, we co-cultured the infected and reporter cells in the presence of AZT. The former alternative would be insensitive to AZT, while the latter would be sensitive to AZT. AZT at 100 nM had a negligible effect on luciferase activity (data not

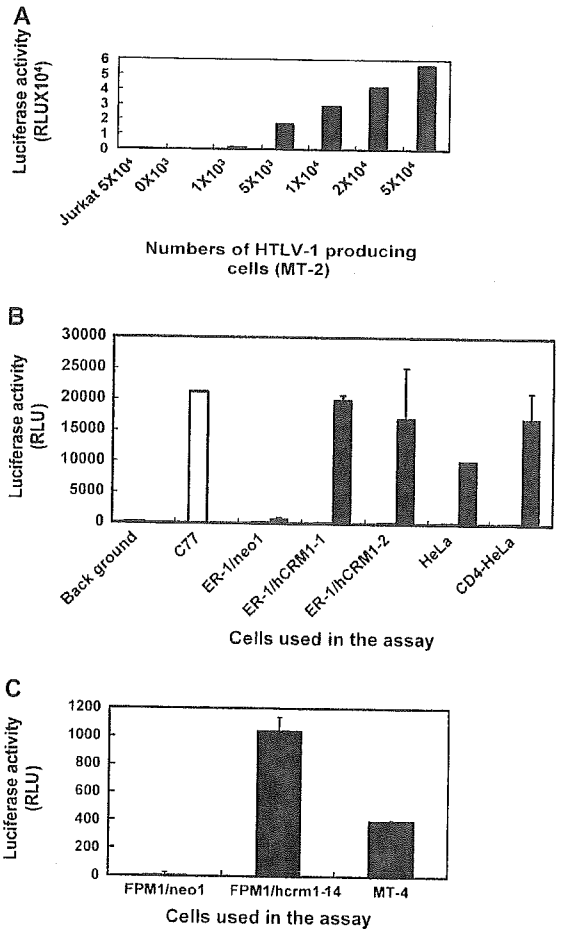

Fig. 4. Env proteins expressed in the rat cells are fusogenic. (A) Various numbers of MT-2 cells were co-cultured with 1×10^5 of the reporter cell 293T/LTR-Luc8. One-fourth of the cell lysate was for the luciferase assay. RLU, relative light units. (B) Luciferase activity induced in reporter cells co-cultured with the HTLV-1 K30-transfected rat and human cells. The results are shown as the mean of three independent experiments. (C) Luciferase activity in the reporter cells co-cultured with HTLV-1 producing rat and human T cells. The results are shown as the mean of two independent experiments.

shown), consistent with poor formation of HTLV-1 infectious virus.

3.4. Efficient early events of HTLV-1 replication in rat cells

To determine the efficiency of early replication events, from entry to the genome integration step, human and rat cells were infected with VSV G-pseudotyped HTLV-1 virus containing the GFP-luciferase gene. ER-1/neo1 and ER1/hCRM1-2 cells produced luciferase signals similar to 293 and 293T cells (Table 3, Experiment 1). Unexpectedly, HeLa and CD4-HeLa cells produced much weaker signals. Luciferase activity was inhibited by the reverse transcriptase inhibitor AZT, indicating that luciferase expression occurred as a result of retrovirus replication, implying reverse-transcription and integration. We next compared the efficiency of the early events

Table 3
Transduction efficiencies of pseudotyped HTLV-1 to various cells

Cells	Luciferase activity (RLU)	
	Without AZT	With AZT
Experiment 1[a]		
ER-1/neo1	3320	228
ER-1/hCRM1-2	2798	126
HeLa	98	103
CD4-HeLa	175	308
293	1946	197
293T	4485	293
Experiment 2[b]		
FPM1	995	275
FPM1/hCRM1-14	465	132
Nb2	860	156
MT-4	2908	416
Jurkat	758	307
Molt-4	884	300

[a] Filtered supernatant of 293T cotransfected with pCMVHT-Δenv, pHTC-GFP-Luc, and pMD-VSV-G were applied to infect 1×10^5 adherent cells. The p19 in the supernatant was 19 ng/ml. Representative results of two independent experiments are shown.

[b] The filtered supernatant was ultra-centrifuged at 14,000 rpm for 90 min. The pellet resultant was suspended in 100 μl of fresh medium, and used to infect the rat and human cells.

in rat T cells with those in human T cells. As shown in Table 3 Experiment 2, both HTLV-1-uninfected (Nb2) and infected rat T cells (FPM1) induced luciferase as much as the human T cells. These results suggest that the early events of HTLV-1 infection indeed occurred in the rat cells at the same or slightly higher levels than in human cells. Free HTLV-1 viruses prepared from feline HTLV-1 producing C77 cells were used to infect activated primary T cells prepared from human PBMC or rat spleen. PCR was used to detect the pX region of HTLV-1 in genomic DNA, extracted from the cells 3 days after infection. We found more intensive signals in the rat T cell samples than the human samples (data not shown). This result supports the above notion, although it is not a quantitative method.

4. Discussion

Previously, we have shown that rCRM1, even though it is able to export Rex protein from the nucleus, does not support Rex multimerization, resulting in poor export of HTLV-1 RNAs in rat cells [33,34]. In this study, we demonstrated that the expression of hCRM1 at physiological levels in rat cells, including epithelial and $CD4^+$ T cells, is not harmful to cell growth, but augments the synthesis of HTLV-1 Gag and Env proteins to levels similar to those seen in human cells. The endogenous rCRM1 does not inhibit the function of Rex, although rCRM1 overexpressed by transfection has been reported to act as a dominant negative inhibitor of hCRM1 function [33]. The Gag precursor synthesized in hCRM1 expressing rat cells is normally processed to the mature p24 and possibly other Gag proteins and then released into the culture medium as sedimentable viral particles, with

an efficiency comparable to human cell lines. The fact that only 25–30% of the Gag protein detected in the medium of both human and rat cells was sedimentable suggests that only a fraction of the Gag proteins may be incorporated into virions, or that the non-sedimentable Gag proteins may reflect the fragility of the virus. Finally, the results using the HTLV-1 pseudovirus [38] suggest that HTLV-1 virions released from the rat cells may have the same infectivity as those released from human cells.

A major route for the spread of HTLV-1 is cell to cell infection mediated by cell fusion caused by the Env proteins in cooperation with the cell adhesion molecules ICAM-1, ICAM-3, and VCAM [48,49]. Some reports suggest that the main function of the Env protein is to mediate cell fusion. These data led us to develop a reporter cell line to quantify Env-mediated cell fusion, based on activation of an HTLV-1 LTR-driven luciferase gene. This system can detect fusion events between as little as approximately 1×10^3 MT-2 cells and 1×10^4 K30-infected cells. Given that this fusion has been shown to be dependent on the Env protein, quantitation of functional Env proteins by this system should be much more sensitive than Western blotting, which requires Env protein concentrated by Con A Sepharose from at least 5×10^5 K30-infected cells. Using this system, we demonstrated that hCRM1 expressing rat cells infected with HTLV-1 mediate cell fusion as efficiently as human cell lines. The results suggest that the fusion capacity of human and rat cells is proportional to the amount of the Env gp46 protein detected by Western blotting (compare Figs. 2, 3 and 4), and indicates that the Env expressed on rat cells is fully fusogenic, which is the basis for HTLV-1 cell to cell transmission.

The poor replication of HTLV-1 in rat cells is unlikely to be related to efficiency of viral entry, since HTLV-1 has a broad host range of infection using Env-coated virus systems [29–31]. The results of our cell fusion-dependent reporter assay (Fig. 4) are consistent with these observations and with the data suggesting that the ubiquitously expressed Glut-1 acts as a HTLV-1 receptor [32]. The post entry steps, including reverse-transcription, nuclear entry, and integration of the HTLV-1 genome, should not be severely inhibited in rat cells since our results using the HTLV-1 pseudovirus system [9] indicate that the infected rat cells induced luciferase, a quantitative marker for successful integration of the viral genome, at levels similar to human cells. Moreover, the early viral proteins, such as Tax and Rex, which are expressed independently of Rex function, are efficiently synthesized in rat cells (Figs. 2 and 3) [44]. Our results suggest that rat cells do not have serious blockages in viral replication other than rCRM1 in the late stage.

In conclusion, rCRM1 can be considered a major species-specific barrier for HTLV-1 replication in rat cells. This barrier is unique to HTLV-1, since, for many viruses, this restriction is determined by species-specific receptor interactions. The fact that expression of hCRM1 allows rat cells to produce high amounts of fully functional Gag and Env proteins and assemble infectious HTLV-1 suggests the feasibility of constructing a transgenic rat expressing hCRM1, which could present a better animal model to study HTLV-1 infection and develop preventive and therapeutic intervention strategies.

Uncited Reference

[41]

Acknowledgements

We thank the NIH AIDS research and reference reagent program for providing HTLV-1 K30, Dr David Derse for the gift of pCMVHT-Δ Env and pHTC-GFP-Luc, and Dr Jun-ichi Fujisawa for providing pLTR-GL3.

References

[1] Y. Hinuma, K. Nagata, M. Hanaoka, M. Nakai, T. Matsumoto, K.I. Kinoshita, S. Shirakawa, I. Miyoshi, Adult T-cell leukemia: antigen in an ATL cell line and detection of antibodies to the antigen in human sera, Proc. Natl. Acad. Sci. U.S.A. 78 (1981) 6476–6480.
[2] M. Osame, K. Usuku, S. Izumo, N. Ijichi, H. Amitani, A. Igata, M. Matsumoto, M. Tara, HTLV-I associated myelopathy, a new clinical entity, Lancet 1 (1986) 1031–1032.
[3] G. Franchini, Molecular mechanisms of human T-cell leukemia/lymphotropic virus type I infection, Blood 86 (1995) 3619–3639.
[4] M. Yoshida, Multiple viral strategies of HTLV-1 for dysregulation of cell growth control, Annu. Rev. Immunol. 19 (2001) 475–496.
[5] M. Hidaka, J. Inoue, M. Yoshida, M. Seiki, Post-transcriptional regulator (rex) of HTLV-1 initiates expression of viral structural proteins but suppresses expression of regulatory proteins, EMBO J. 7 (1988) 519–523.
[6] B.R. Cullen, Regulation of human immunodeficiency virus replication, Annu. Rev. Microbiol. 45 (1991) 219–250.
[7] J. Inoue, M. Yoshida, M. Seiki, Transcriptional (p40x) and post-transcriptional (p27x-III) regulators are required for the expression and replication of human T-cell leukemia virus type I genes, Proc. Natl. Acad. Sci. U.S.A. 84 (1987) 3653–3657.
[8] C. Ballaun, G.K. Farrington, M. Dobrovnik, J. Rusche, J. Hauber, E. Bohslein, Functional analysis of human T-cell leukemia virus type I rex-response element: direct RNA binding of Rex protein correlates with in vivo activity, J. Virol. 65 (1991) 4408–4413.
[9] H.P. Bogerd, G.L. Huckaby, Y.F. Ahmed, S.M. Hanly, W.C. Greene, The type I human T-cell leukemia virus (HTLV-I) Rex trans-activator binds directly to the HTLV-I Rex and the type 1 human immunodeficiency virus Rev RNA response elements, Proc. Natl. Acad. Sci. U.S.A. 88 (1991) 5704–5708.
[10] M. Fornerod, M. Ohno, M. Yoshida, I.W. Mattaj, CRM1 is an export receptor for leucine-rich nuclear export signals, Cell 90 (1997) 1051–1060.
[11] Y. Hakata, T. Umemoto, S. Matsushita, H. Shida, Involvement of human CRM1 (exportin 1) in the export and multimerization of the Rex protein of human T-cell leukemia virus type 1, J. Virol. 72 (1998) 6602–6607.
[12] M.E. Nemergut, M.E. Lindsay, A.M. Brownawell, I.G. Macara, Ran-binding protein 3 links Crm1 to the Ran guanine nucleotide exchange factor, J. Biol. Chem. 277 (2002) 17385–17388.
[13] H. Bogerd, W.C. Greene, Dominant negative mutants of human T-cell leukemia virus type I Rex and human immunodeficiency virus type 1 Rev fail to multimerize in vivo, J. Virol. 67 (1993) 2496–2502.
[14] H. Shida, Y. Hakata, Multiple roles of cellular export machinery in HTLV-1 Rex functioning, Gann monogr. 50 (2003) 61–72.
[15] H. Shida, T. Tochikura, T. Sato, T. Konno, K. Hirayoshi, M. Seki, Y. Ito, M. Hatanaka, Y. Hinuma, M. Sugimoto, et al., Effect of the recombinant vaccinia viruses that express HTLV-I envelope gene on HTLV-I infection, EMBO J. 6 (1987) 3379–3384.

[16] K. Ogawa, S. Matsuda, A. Seto, Induction of leukemic infiltration by allogeneic transfer of HTLV-I-transformed T cells in rabbits, Leuk. Res. 13 (1989) 399–406.
[17] Y. Tanaka, R. Tanaka, E. Terada, Y. Koyanagi, N. Miyano-Kurosaki, N. Yamamoto, E. Baba, M. Nakamura, H. Shida, Induction of antibody responses that neutralize human T-cell leukemia virus type I infection in vitro and in vivo by peptide immunization, J. Virol. 68 (1994) 6323–6331.
[18] M. Kazanji, A. Ureta-Vidal, S. Ozden, F. Tangy, B. de Thoisy, L. Fiette, A. Talarmin, A. Gessain, G. de, The Lymphoid organs as a major reservoir for human T-cell leukemia virus type 1 in experimentally infected squirrel monkeys (*Saimiri sciureus*): provirus expression, persistence, and humoral and cellular immune responses, J. Virol. 74 (2000) 4860–4867.
[19] T.M. McGinn, Q. Wei, J. Stallworth, P.N. Fultz, Immune responses to HTLV-I(ACH) during acute infection of pig-tailed macaques, AIDS Res. Hum. Retroviruses 20 (2004) 443–456.
[20] K. Ibuki, S.I. Funahashi, H. Yamamoto, M. Nakamura, T. Igarashi, T. Miura, E. Ido, M. Hayami, H. Shida, Long-term persistence of protective immunity in cynomolgus monkeys immunized with a recombinant vaccinia virus expressing the human T cell leukaemia virus type I envelope gene, J. Gen. Virol. 78 (Pt 1) (1997) 147–152.
[21] R. Feng, A. Kabayama, K. Uchida, H. Hoshino, M. Miwa, Cell-free entry of human T-cell leukemia virus type I to mouse cells, Jpn. J. Cancer Res. 92 (2001) 410–416.
[22] C. Denesvre, P. Sonigo, A. Corbin, H. Ellerbrok, M. Sitbon, Influence of transmembrane domains on the fusogenic abilities of human and murine leukemia retrovirus envelopes, J. Virol. 69 (1995) 4149–4157.
[23] K. Nagy, P. Clapham, R. Cheingsong-Popov, R.A. Weiss, Human T-cell leukemia virus type I: induction of syncytia and inhibition by patients' sera, Int. J. Cancer 32 (1983) 321–328.
[24] B. Sun, T. Nitta, M. Shoda, M. Tanaka, S. Hanai, H. Hoshino, M. Miwa, Cell-free human T-cell leukemia virus type I binds to, and efficiently enters mouse cells, Jpn. J. Cancer Res. 93 (2002) 760–766.
[25] F. Ibrahim, L. Fiette, A. Gessain, N. Buisson, G. de-The, R. Bomford, Infection of rats with human T-cell leukemia virus type-I: susceptibility of inbred strains, antibody response and provirus location, Int. J. Cancer 58 (1994) 446–451.
[26] T. Suga, T. Kameyama, T. Kinoshita, K. Shimotohno, M. Matsumura, H. Tanaka, S. Kushida, Y. Ami, M. Uchida, K. Uchida, et al., Infection of rats with HTLV-1: a small-animal model for HTLV-I carriers, Int. J. Cancer 49 (1991) 764–769.
[27] N. Ishiguro, M. Abe, K. Seto, H. Sakurai, H. Ikeda, A. Wakisaka, T. Togashi, M. Tateno, T. Yoshiki, A rat model of human T lymphocyte virus type I (HTLV-I) infection. I. Humoral antibody response, provirus integration, and HTLV-I-associated myelopathy/tropical spastic paraparesis-like myelopathy in seronegative HTLV-I carrier rats, J. Exp. Med. 176 (1992) 981–989.
[28] T. Kasai, H. Ikeda, U. Tomaru, I. Yamashita, O. Ohya, K. Morita, A. Wakisaka, E. Matsuoka, T. Moritoyo, K. Hashimoto, I. Higuchi, S. Izumo, M. Osame, T. Yoshiki, A rat model of human T lymphocyte virus type I (HTLV-I) infection: in situ detection of HTLV-I provirus DNA in microglia/macrophages in affected spinal cords of rats with HTLV-I-induced chronic progressive myeloneuropathy, Acta. Neuropathol. (Berl) 97 (1999) 107–112.
[29] Q.X. Li, D. Camerini, Y. Xie, M. Greenwald, D.R. Kuritzkes, I.S. Chen, Syncytium formation by recombinant HTLV-II envelope glycoprotein, Virology 218 (1996) 279–284.
[30] R.E. Sutton, D.R. Littman, Broad host range of human T-cell leukemia virus type 1 demonstrated with an improved pseudotyping system, J. Virol. 70 (1996) 7322–7326.
[31] K. Okuma, M. Nakamura, S. Nakano, Y. Niho, Y. Matsuura, Host range of human T-cell leukemia virus type I analyzed by a cell fusion-dependent reporter gene activation assay, Virology 254 (1999) 235–244.
[32] N. Manel, F.J. Kim, S. Kinet, N. Taylor, M. Sitbon, J.L. Battini, The ubiquitous glucose transporter GLUT-1 is a receptor for HTLV, Cell 115 (2003) 449–459.
[33] Y. Hakata, M. Yamada, H. Shida, Rat CRM1 is responsible for the poor activity of human T-cell leukemia virus type 1 Rex protein in rat cells, J. Virol. 75 (2001) 11515–11525.
[34] Y. Hakata, M. Yamada, H. Shida, A multifunctional domain in human CRM1 (exportin 1) mediates RanBP3 binding and multimerization of human T-cell leukemia virus type 1 Rex protein, Mol. Cell. Biol. 2 (2003) 8751–8761.
[35] M. Callanan, N. Kudo, S. Gout, M. Brocard, M. Yoshida, S. Dimitrov, S. Khochbin, Developmentally regulated activity of CRM1/XPO1 during early Xenopus embryogenesis, J. Cell Sci. 113 (Pt 3) (2000) 451–459.
[36] M. Stremlau, C.M. Owens, M.J. Perron, M. Kiessling, P. Autissier, J. Sodroski, The cytoplasmic body component TRIM5alpha restricts HIV-1 infection in Old World monkeys, Nature 427 (2004) 848–853.
[37] A.M. Sheehy, N.C. Gaddis, J.D. Choi, M.H. Malim, Isolation of a human gene that inhibits HIV-1 infection and is suppressed by the viral Vif protein, Nature 418 (2002) 646–650.
[38] D. Derse, S.A. Hill, P.A. Lloyd, H. Chung, B.A. Morse, Examining human T-lymphotropic virus type 1 infection and replication by cell-free infection with recombinant virus vectors, J. Virol. 75 (2001) 8461–8468.
[39] N. Fan, J. Gavalchin, B. Paul, K.H. Wells, M.J. Lane, B.J. Poiesz, Infection of peripheral blood mononuclear cells and cell lines by cell-free human T-cell lymphoma/leukemia virus type I, J. Clin. Microbiol. 30 (1992) 905–910.
[40] M. Onishi, S. Kinoshita, Y. Morikawa, A. Shibuya, J. Phillips, L.L. .Lanier, D.M. Gorman, G.P. Nolan, A. Miyajima, T. Kitamura, Application of retrovirus-mediated expression cloning, Exp. Hematol. 24 (1996) 324–329.
[41] J. Fujisawa, M. Seiki, T. Kiyokawa, M. Yoshida, Functional activation of the long terminal repeat of human T-cell leukemia virus type I by a trans-acting factor, Proc. Natl. Acad. Sci. U.S.A. 82 (1985) 2277–2281.
[42] Y. Tanaka, M. Yasumoto, H. Nyunoya, T. Ogura, M. Kikuchi, K. Shimotohno, H. Shiraki, N. Kuroda, H. Shida, H. Tozawa, Generation and characterization of monoclonal antibodies against multiple epitopes on the C-terminal half of envelope gp46 of human T-cell leukemia virus type-I (HTLV-I), Int. J. Cancer 46 (1990) 675–681.
[43] Y. Tanaka, L. Zeng, H. Shiraki, H. Shida, H. Tozawa, Identification of a neutralization epitope on the envelope gp46 antigen of human T cell leukemia virus type I and induction of neutralizing antibody by peptide immunization, J. Immunol. 147 (1991) 354–360.
[44] Y. Koya, T. Ohashi, H. Kato, S. Hanabuchi, T. Tsukahara, F. Takemura, K. Etoh, M. Matsuoka, M. Fujii, M. Kannagi, Establishment of a seronegative human T-cell leukemia virus type 1 (HTLV-1) carrier state in rats inoculated with a syngeneic HTLV-1-immortalized T-cell line preferentially expressing Tax, J. Virol. 73 (1999) 6436–6443.
[45] N. Yamamoto, M. Okada, Y. Koyanagi, M. Kannagi, Y. Hinuma, Transformation of human leukocytes by cocultivation with an adult T cell leukemia Virus producer cell line, Science 217 (1982) 737–739.
[46] M. Popovic, P.S. Sarin, M. Robert-Gurroff, V.S. Kalyanaraman, D. Mann, J. Minowada, R.C. Gallo, Isolation and transmission of human retrovirus (human t-cell leukemia virus), Science 219 (1983) 856–859.
[47] L. Delamarre, A.R. Rosenberg, C. Pique, D. Pham, M.C. Dokhelar, A novel human T-leukemia virus type 1 cell-to-cell transmission assay permits definition of SU glycoprotein amino acids important for infectivity, J. Virol. 71 (1997) 259–266.
[48] S.R. Jassal, M.D. Lairmore, A.J. Leigh-Brown, D.W. Brighty, Soluble recombinant HTLV-1 surface glycoprotein competitively inhibits syncytia formation and viral infection of cells, Virus. Res. 78 (2001) 17–34.
[49] J.E. Hildreth, A. Subramanium, R.A. Hampton, Human T-cell lymphotropic virus type 1 (HTLV-1)-induced syncytium formation mediated by vascular cell adhesion molecule-1: evidence for involvement of cell adhesion molecules in HTLV-1 biology, J. Virol. 71 (1997) 1173–1180.
[50] S. Daenke, S.A. McCracken, S. Booth, Human T-cell leukaemia/lymphoma virus type 1 syncytium formation is regulated in a cell-specific manner by ICAM-1, ICAM-3 and VCAM-1 and can be inhibited by antibodies to integrin beta2 or beta7, J. Gen. Virol. 80 (Pt 6) (1991) 429–436.

JOURNAL OF VIROLOGY, Feb. 2005, p. 2087–2096 Vol. 79, No. 4
0022-538X/05/$08.00+0 doi:10.1128/JVI.79.4.2087–2096.2005

Potent Anti-R5 Human Immunodeficiency Virus Type 1 Effects of a CCR5 Antagonist, AK602/ONO4128/GW873140, in a Novel Human Peripheral Blood Mononuclear Cell Nonobese Diabetic-SCID, Interleukin-2 Receptor γ-Chain-Knocked-Out AIDS Mouse Model

Hirotomo Nakata,[1] Kenji Maeda,[1] Toshikazu Miyakawa,[1] Shiro Shibayama,[2] Masayoshi Matsuo,[2] Yoshikazu Takaoka,[2] Mamoru Ito,[3] Yoshio Koyanagi,[4]† and Hiroaki Mitsuya[1,5]*

Department of Infectious Diseases, Kumamoto University Graduate School of Medicine, Kumamoto,[1] Ono Pharmaceutical Co. Ltd., Osaka,[2] Central Institute for Experimental Animals, Kawasaki,[3] Department of Virology, Tohoku University Graduate School of Medicine, Sendai,[4] Japan, and Experimental Retrovirology Section, HIV and AIDS Malignancy Branch, National Cancer Institute, Bethesda, Maryland[5]

Received 27 May 2004/Accepted 1 October 2004

We established human peripheral blood mononuclear cell (PBMC)-transplanted R5 human immunodeficiency virus type 1 isolate JR-FL (HIV-1_{JR-FL})-infected, nonobese diabetic-SCID, interleukin 2 receptor γ-chain-knocked-out (NOG) mice, in which massive and systemic HIV-1 infection occurred. The susceptibility of the implanted PBMC to the infectivity and cytopathic effect of R5 HIV-1 appeared to stem from hyperactivation of the PBMC, which rapidly proliferated and expressed high levels of CCR5. When a novel spirodiketopiperazine-containing CCR5 inhibitor, AK602/ONO4128/GW873140 (molecular weight, 614), was administered to the NOG mice 1 day after R5 HIV-1 inoculation, the replication and cytopathic effects of R5 HIV-1 were significantly suppressed. In saline-treated mice ($n = 7$), the mean human $CD4^+/CD8^+$ cell ratio was 0.1 on day 16 after inoculation, while levels in mice ($n = 8$) administered AK602 had a mean value of 0.92, comparable to levels in uninfected mice ($n = 7$). The mean number of HIV-RNA copies in plasma in saline-treated mice were $\sim 10^6$/ml on day 16, while levels in AK602-treated mice were 1.27×10^3/ml ($P = 0.001$). AK602 also significantly suppressed the number of proviral DNA copies and serum p24 levels ($P = 0.001$). These data suggest that the present NOG mouse system should serve as a small-animal AIDS model and warrant that AK602 be further developed as a potential therapeutic for HIV-1 infection.

Highly active antiretroviral therapy has brought about a major impact on the AIDS epidemics in the industrially advanced nations (5, 22). However, eradication of human immunodeficiency virus type 1 (HIV-1) is thought to be currently impossible, due in part to the viral reservoirs remaining in blood and infected tissues (6). The limitation of antiviral therapy of AIDS is exacerbated by complicated regimens, the development of drug-resistant HIV-1 variants (11), and a number of inherent adverse effects (2, 31). Hence, the identification of new antiretroviral drugs that have unique mechanisms of action and produce no or minimal adverse effects remains an important therapeutic objective. In regard to development of potential anti-HIV therapies or vaccines, experimental animal models for AIDS which allow the determination of the possible efficacy of antiviral agents or vaccines have been sought since severe combined immunodeficiency (SCID) mice engrafted with human fetal thymus, liver, or peripheral blood mononuclear cells (PBMC) were first exploited to examine antiretroviral agents (19, 25). However, a number of mouse models have suffered from false-positive and false-negative results in detecting or quantifying HIV-1 infection and replication and have required a large number of samples and mice for testing (25, 29).

In the present work, we established human PBMC-transplanted R5 HIV-1_{JR-FL}-infected, nonobese diabetic (NOD)-SCID, interleukin 2 receptor γ (IL-2Rγ)-chain-knocked-out (NOG) mice, in which massive and systemic HIV-1 infection occurs, human $CD4^+/CD8^+$ cell ratios significantly decrease, and high levels of R5 HIV-1 viremia reaching as high as 10^6 copies/ml are achieved. Furthermore, we demonstrated that this unprecedented susceptibility of the implanted human PBMC to the infectivity and cytopathic effects of R5 HIV-1 infection stems from hyperactivation of the PBMC. Here, we also report a novel small nonpeptide CCR5 antagonist, AK602/ONO4128/GW873140, which exerts potent anti-HIV-1 activity in vitro against laboratory and clinical strains of HIV-1, including highly multidrug-resistant (MDR) variants.

* Corresponding author. Mailing address: Department of Infectious Diseases, Kumamoto University Graduate School of Medicine, 1-1-1 Honjo, Kumamoto 860-8556, Japan. Phone: 81-96-373-5156. Fax: 81-96-363-5265. E-mail: hmitsuya@helix.nih.gov.

† Present address: Laboratory of Viral Pathogenesis, Institute for Virus Research, Kyoto University, Kyoto 606-8507, Japan.

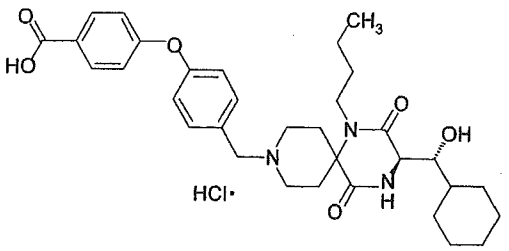

FIG. 1. Structure of AK602.

MATERIALS AND METHODS

Transplantation of human PBMC in NOG mice. NOD-SCID (NOG) mice (10, 33) were maintained in the Central Institute for Experimental Animals (Kawasaki, Japan). Mice were 4 to 6 weeks old at the time of transfer of human PBMC. The human PBMC-transplanted NOG (hu-PBMC-NOG) mice were generated by methods previously described (23, 24). Briefly, PBMC (10^7) were freshly prepared from heparinized blood of a single healthy HIV-1-seronegative donor by Ficoll-Hypaque density gradient centrifugation, resuspended in RPMI 1640-based culture medium (0.5 ml), and infused intraperitoneally to each mouse. The experimental protocol was approved by the Ethics Review Committees for Animal Experimentation of the participating institutions.

Assay for proliferation and CCR5 expression of transplanted human PBMC recovered from hu-PBMC-NOG mice. Freshly isolated human PBMC (2×10^7 cells/ml) were incubated in phosphate-buffered saline (PBS) containing 10 μM 5-carboxyfluorescein diacetate succinimidyl ester (CFSE; Molecular Probes, Eugene, Oreg.) for 15 min at 37°C for CFSE labeling as previously described by Lyons (16), washed, and resuspended in RPMI 1640. One part of the labeled PBMC preparation was intraperitoneally injected (10^7 PBMC) to each NOG mouse, and human PBMC were recovered from peritoneal lavages and spleen. The other part of the preparation was immediately stimulated with 10 μg of phytohemagglutinin (PHA)/ml, cultured, and harvested. PBMC samples thus obtained were labeled with phycoerythrin (PE)-conjugated anti-CCR5 monoclonal antibody 3A9 or peridinin chlorophyll protein-conjugated anti-HLA-DR antibody (BD Pharmingen, San Diego, Calif.) and subjected to flow cytometric analysis with a Becton Dickinson FACscan cytometer; the data were analyzed by Cell Quest software (Becton Dickinson, Franklin Lakes, N.J.). A quantitative fluorescence-activated cell sorting (FACS) assay that relies on a series of precalibrated beads that bind to a fixed number of mouse immunoglobulin G molecules (Quantum Simply Cellular Kit; Sigma, Saint Louis, Mo.) to determine the absolute number of CCR5s on the cell surface was also conducted according to the manufacturer's instructions (15).

Cells and viruses. The HeLa-CD4-LTR-β-gal indicator cell line expressing human CCR5 ($CCR5^+$ MAGI) (18), a kind gift from Yosuke Maeda, was used for the present study. 293T cells (a human embryonic kidney cell line) were cultured in Dulbecco's modified Eagle medium supplemented with 10% fetal calf serum (FCS) and antibiotics and used for transfection of DNA plasmid containing the R5 HIV-$1_{JR\text{-}FL}$ genome (13). PBMC isolated from HIV-1-seronegative individuals were cultured with 10% FCS and antibiotics with 10 μg of PHA/ml for 3 days prior to anti-HIV-1 activity assay in vitro (PHA-PBMC). A panel of HIV-1 strains was employed for the drug susceptibility attempt: HIV-$1_{Ba\text{-}L}$ (7), HIV-$1_{JR\text{-}FL}$ (13), HIV-$1_{NL4\text{-}3}$ (32), a wild-type HIV-1_{MOKW} isolated from a drug-naive AIDS patient (17), and MDR primary HIV-1 (HIV-1_{MDR}) strain (HIV-1_{JSL} and HIV-1_{MM}) (35). All primary HIV-1 strains were passaged once or twice in PHA-PBMC cultures and the culture supernatants were stored at −80°C until use. Antiviral assays using PHA-PBMC were conducted as previously reported (12, 17, 35).

Antiviral agents and assay for inhibition of R5 HIV-1 infectivity and replication. A series of different spirodiketopiperazine (SDP) derivatives were newly designed, synthesized, and tested for their activity against in vitro infectivity and replication of R5 HIV-1 as previously described (17). AK602 was chosen for this study based on its CCR5-specific, potent activity against R5 HIV-1. A method for the synthesis of AK602 will be published elsewhere. The structure of AK602 is illustrated in Fig. 1. An approved drug for therapy for HIV-1 infection, 2′,3′-dideoxyinosine (ddI) (20, 21), was kindly provided by Ajinomoto Co., Inc, Tokyo, Japan. TAK779 and SCH-C were synthesized according to previously published data (1, 30). The MAGI assay using $CCR5^+$ MAGI cells was conducted as previously described (17) with minor modifications. Briefly, $CCR5^+$ MAGI cells were seeded in 96-well, flat-bottomed microculture plates (10^4 cells/well) for 24 h, exposed to 0.1 or 1 μM AK602 for 30 min, washed three times, exposed to R5 HIV-1 (100 50% tissue culture infectious doses) at various time points after AK602 removal, and cultured in Dulbecco's modified Eagle medium containing 15% FCS for 48 h. Following the removal of supernatants and lysis of the cells with PBS (100 μl) containing 1% Triton X-100, a solution (100 μl) containing 10 mM chlorophenol red-β-D-galactopyranoside, 2 mM $MgCl_2$, and 0.1 M KH_2PO_4 was added to each well; the mixture was incubated at room temperature in the dark for 30 min; and the optical density (wavelength, 570 nm) was measured with a microplate reader (*V*max, Molecular Devices, Sunnyvale, Calif). All assays were performed in triplicate.

Pharmacokinetic analysis of AK602 in hu-PBMC-NOG mice. Pharmacokinetic analysis of AK602 in hu-PBMC-NOG mice was performed as previously described (28). In brief, plasma samples were collected periodically over 12 h, following a single AK602 administration at a dose of 60 mg/kg of body weight dissolved in 400 μl of 4% hydroxypropyl-β cyclodextrin (HPBC). Each plasma sample (150 μl) was centrifuged at 3,000 rpm for 10 min, and the supernatant was vacuum concentrated and injected into the high-performance liquid chromatography (HPLC) system. The eluent was monitored at 255 nm of UV, and the AK602 concentration in plasma was determined.

Determination of amounts of AK602 persistently bound to CCR5 in hu-PBMC-NOG mice. Blood samples were collected from the tail vein of each hu-PBMC-NOG mouse at various time points following a single intraperitoneal administration of AK602 at a dose of 60 mg/kg. PBMC were isolated by density gradient centrifugation and stained with fluorescein isothiocyanate-conjugated monoclonal antibody 45531 (R&D Systems, Minneapolis, Minn.) specific for the C-terminal half of the second extracellular loop (ECL2B) of CCR5 (15) known to be competitively replaced by SDP derivatives (17) or with PE-conjugated monoclonal antibody 3A9, which binds to the N-terminus extracellular domain of CCR5 (17). PBMC were then subjected to FACS analysis.

Treatment of R5 HIV-1-infected hu-PBMC-NOG mice with anti-HIV-1 agents. Sixteen days after PBMC infusion, the mice were bled from the tail vein, and three-color flow cytometric analysis was performed to confirm positive engraftment of human HLA, CD4, and CD8 antigens on the cells recovered. HIV-$1_{JR\text{-}FL}$ (2,000 50% tissue culture infectious doses) was intraperitoneally inoculated to each mouse in which PBMC engraftment was confirmed. Twenty-four hours after the R5 HIV-1 inoculation, administration of AK602 (120 mg in 4% HPBC/kg/day, twice a day), ddI (50 mg in 4% HPBC/kg/day, twice a day), or saline was implemented and continued by day 16. On days 5 and 9 after the R5 HIV-1 inoculation, blood samples were collected from mouse tail veins for immunologic and virological monitoring (see below). On day 16, blood samples were collected by cardiocentesis, and the mice were sacrificed. The experimental protocol for the treatment is illustrated in Fig. 2.

Immunologic and virological monitoring. Human PBMC recovered from mice were subjected to immunologic and virological monitoring as previously described (23, 24). The $CD4^+/CD8^+$ cell ratios were determined by FACS analysis with PE-conjugated mouse anti-CD4 and peridinin chlorophyll protein-conjugated mouse anti-CD8 (BD Pharmingen) monoclonal antibodies. Determination of HIV-1 DNA copy numbers in recovered human PBMC was performed by real-time PCR assay with Taqman Master mixture (PE Biosystems) and HIV long terminal repeat-specific primers M667 (5′-GGC TAA CTA GGG AAC CCA CTG-3′) and AA55 (5′-CTG CTA GAG ATT TTC CAC ACT GAC-3′). HIV-1-specific products were quantified with the ABI 7700 detection system (Applied Biosystems, Foster City, Calif.), and cell numbers were determined with the RAG-1 gene. The numbers of $CD4^+$ cells were calculated based on the percentage of $CD4^+$ values obtained from the FACS analysis of each test PBMC sample, and R5 HIV-1 proviral DNA copy numbers were expressed as copy numbers per 10^5 $CD4^+$ cells. In some experiments, $CD4^+$ and $CD4^-$ cells were separated before real-time PCR assay with the rapid immunomagnetic CD4-positive cell isolation kit (Dynabeads M-450 CD4; Dynal Biotech, Inc., Lake

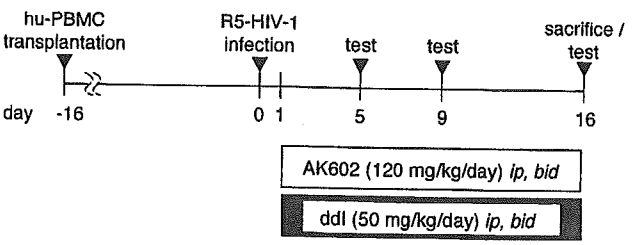

FIG. 2. Protocol for drug administration and immunological and virologic monitoring.

Success, N.Y.). The amounts of p24 antigen in murine sera were determined using a fully automated chemiluminescent enzyme immunoassay system (Lumipulse F; Fujirebio, Inc., Tokyo, Japan) as previously described (12). Plasma viral load was quantified with the AMPLICOR HIV-1 monitor test kit, version 1.5 (Roche Diagnostics, Branchburg, N.J.).

Statistical analyses. Nonparametric statistical analyses were performed by using the Mann-Whitney U test (Statview, version 5.0; Abacus Concepts, Berkeley, Calif.). The difference between viremia levels in two groups of mice was determined by the Wilcoxon rank sum test. For each mouse, the value of $\log_{10}$ RNA copies was calculated, and the slope corresponding to the rate of increase per day was determined by simple linear regression for the days (5, 9, and 16) of blood collection. The resulting slopes for all mice in the untreated groups were compared to the slopes of mice in each of the other two groups.

RESULTS

Transplanted PBMC in hu-PBMC-NOG mice are intensely activated and express high levels of CCR5. When we examined the proliferation profile of PBMC stimulated with PHA in vitro by treatment with the vital dye CFSE, which allows the analysis of cell proliferation as the CFSE's fluorescence intensity is halved per each cell division, there was only a slight shift to the left in the flow cytometric profile on days 1 and 2 of culture (Fig. 3A). On day 4 of culture, a discrete shift to the left was identified, suggesting that the PHA-PBMC underwent up to four cycles of proliferation in vitro by day 4. In contrast, PBMC transplanted and recovered on day 2 had apparently undergone ~4 cycles of proliferation; by day 4, a majority of cells had undergone up to 10 cycles and beyond in proliferation (Fig. 3B). It was possible that the CFSE-negative and weakly CFSE-positive cells which accumulated on days 2 and 4 (Fig. 3B) were murine cells that engulfed and degraded CFSE. We therefore conducted experiments in which the cells with CFSE dilution were directly confirmed to be human CCR5-positive cells. As can be seen in Fig. 3C, when cells were recovered from the spleen of an NOG mouse into which CFSE-labeled PBMC had been transplanted and stained with monoclonal antibody 45531, which is specific for the C-terminal half of the second extracellular loop (ECL2B) of CCR5 (15), the majority of such human $CCR5^+$ cells proved to be CFSE negative. We also examined the levels of cellular activation by the expression of HLA-DR on cell surface. The levels of HLA-DR expression in PBMC recovered from uninfected NOG mice 3 days after transplantation were much greater than those in 3-day-cultured PBMC following PHA stimulation (Fig. 3D). The fluorescence intensity in the same donor's PHA-PBMC examined on three different occasions was 21 ± 4, while that of the PBMC recovered from mice was 91 ± 25 (Fig. 3D). When we further assessed the levels of CCR5 expression, the PBMC recovered from the mice on day 3 proved to be strongly positive for CCR5 (Fig. 3E). The CCR5-positive fraction in the PBMC recovered was 49.7%, while that in PHA-PBMC was 27.3%. The mean fluorescence intensity of the $CCR5^+$ cell population was 141, compared to the $CCR5^+$ cell population in PHA-PBMC with a mean fluorescence intensity of 51. The estimated number of CCR5 expressed on the PBMC recovered on day 3 was 25,348 (as antibody binding sites per cell) while that on PHA-PBMC on day 3 in culture was 8,981 antibody binding sites as examined by quantitative FACS assay. These data indicate that the transplanted human PBMC were intensely activated and rapidly proliferating and expressed high levels of CCR5 on their cell surfaces.

Potent activity of AK602 against R5 HIV-1 in vitro. Among SDP derivatives we designed and synthesized, AK602 was identified to be highly potent against a broad spectrum of R5 HIV-1 strains, including MDR clinical R5 HIV-1 isolates in vitro with 50% inhibitory concentration (IC_{50}) values of 0.3 to 0.6 nM, although two previously published CCR5 antagonists (TAK779 and SCH-C) were substantially less potent than AK602 (Table 1). AK602 and other CCR5 antagonists failed to inhibit the replication of an X4 HIV-1 strain, HIV-1_{NL4-3}.

Pharmacokinetics of AK602 in hu-PBMC-NOG mice. We examined the pharmacokinetics of AK602 in hu-PBMC-NOG mice by intraperitoneally administering the compound at a dose of 60 mg/kg. Plasma samples were collected periodically up to 12 h and subjected to HPLC analysis. As shown in Fig. 4A, the concentration of AK602 reached the maximal concentration immediately after intraperitoneal administration and decreased rapidly. The calculated plasma half-life in the α-phase of the concentration curve was as short as 29 min.

AK602 persists on cell surface CCR5. As shown above, the plasma half-life of AK602 turned out to be short; however, considering that AK602 possesses such a high affinity to CCR5 and potent activity against R5 HIV-1 in vitro, it was thought possible that AK602 would remain attached on cellular CCR5 for an extensive period of time and exert anti-R5 HIV-1 activity even when the compound was depleted from circulation. To examine this possibility, we used two monoclonal antibodies, 45531 and 3A9. When human PBMC were recovered from a hu-PBMC-NOG mouse 2 and 6 h after AK602 administration (60 mg/kg) and stained with 45531, AK602 proved to block the binding of 45531 to CCR5 (Fig. 4B), while AK602 failed to block 3A9 binding to CCR5 (Fig. 4C), suggesting that AK602 did not elicit CCR5 internalization or shedding at all at least for 6 h. We subsequently examined whether AK602 remained on cellular CCR5 with the 45531 monoclonal antibody. When the cells were recovered from mice 2, 6, and 14 h after the AK602 administration, the mean values of the percentage of AK602 occupancy were 85 (four mice), 54 (three mice), and 16 (three mice), respectively. It was calculated that it took about 9 h for AK602 occupancy to be reduced by 50% (Fig. 4D).

Anti-R5 HIV-1 activity of AK602 persistently seen after its removal from culture medium. In another depletion experiment, we exposed $CCR5^+$ MAGI cells to AK602 for 30 min, depleted the compound from the culture by thorough washing, incubated the cells for various lengths of time, exposed the cells to HIV-1_{Ba-L}, further cultured the cells for 48 h, and determined whether HIV-1_{Ba-L} infection was blocked by AK602 exposure (Fig. 4E). When the $CCR5^+$ MAGI cells were exposed to 0.1 and 1 μM AK602 and exposed to HIV-1_{Ba-L} immediately afterward, the values for protection were 68 and 85%, respectively. When the cells were exposed to HIV-1_{Ba-L} 4 h after depletion, 49 and 72% of the cells were protected by 0.1 and 1 μM AK602. When the cells were exposed to HIV-1_{Ba-L} 12 and 24 h after depletion, 57 and 45% of the cells were seen protected by 1 μM, respectively (Fig. 4E).

Effects of AK602 on $CD4^+$ and $CD8^+$ cell counts in R5 HIV-1-infected hu-PBMC-NOG mice. PBMC were recovered from murine blood samples collected on days 5, 9, and 16 after R5 HIV-1 inoculation and subjected to flow cytometric analysis for determination of $CD4^+/CD8^+$ cell ratios. As shown in Fig. 5A, in PBMC recovered on day 16 from a representative

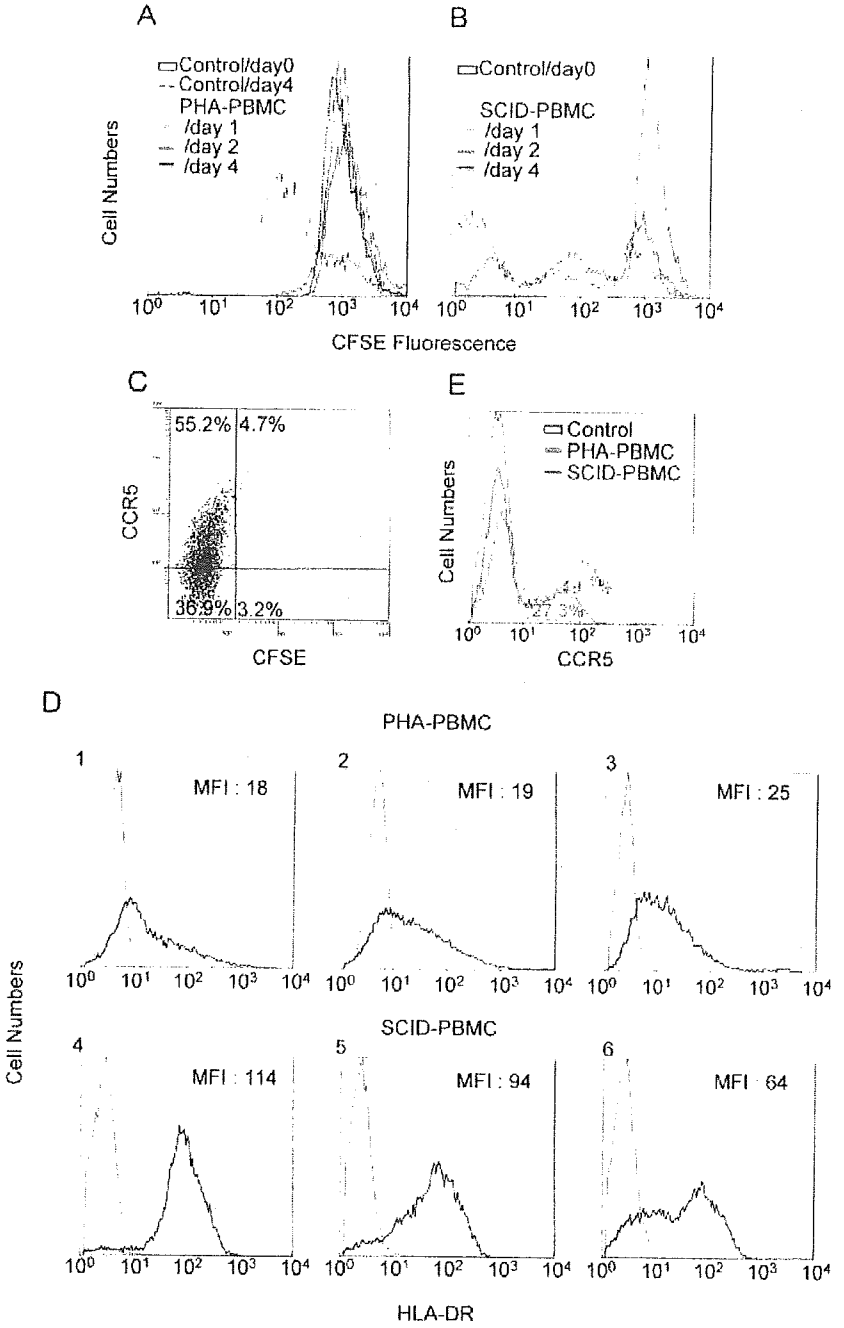

FIG. 3. Transplanted PBMC are intensely activated and express high levels of CCR5. (A and B) Proliferation profiles of PHA-PBMC and transplanted and recovered PBMC. Freshly prepared PBMC were incubated with the vital dye CFSE, and one part of such PBMC preparation was stimulated with PHA, while the other part was intraperitoneally transplanted to mice. On days 1, 2, and 4, the cells were harvested and the fluorescence intensity of CFSE was determined. Note that transplanted PBMC recovered on day 2 had undergone ~4 cycles of proliferation; by day 4, a majority of cells had undergone ~10 cycles and more of proliferation. (C) CCR5 expression level and CFSE intensity in human PBMC harvested from a spleen of hu-PBMC-NOG mouse on day 4. (D) Intense activation of PBMC after transplantation. PBMC stimulated with PHA and cultured for 4 days (panels 1 to 3) and transplanted PBMC recovered from the uninfected mice on day 4 (panels 4 to 6) were stained with an anti-HLA-DR monoclonal antibody. Note that HLA-DR expression levels in transplanted PBMC were much higher than those in PHA-PBMC. (E) CCR5 expression profiles of PHA-PBMC and transplanted PBMC. PBMC stimulated with PHA and cultured for 3 days and transplanted PBMC recovered from the uninfected mice on day 3 were stained with PE-conjugated anti-CCR5 monoclonal antibody 3A9 and subjected to flow cytometric analysis. SCID-PBMC, PBMC transplanted and recovered.

R5 HIV-1-infected, saline-treated mouse, there were only few $CD4^+$ cells (3.9% [1.4% + 2.5%]) resulting in a $CD4^+/CD8^+$ cell ratio of 0.05. However, a distinct $CD4^+$ cell population (55.1% [4.4% + 50.7%]) resulting in a $CD4^+/CD8^+$ ratio of 1.84 (Fig. 5B) was seen in PBMC recovered from an AK602-treated mouse, and the size of this $CD4^+$ cell population was comparable to that seen in a ddI-treated mouse (53.2% [3.8% + 49.4%]) and that in an uninfected mouse (48.9% [3.8% +